Response to reviewers' comments

We thank the reviewers for taking the time to provide us with thorough set of reviews for the paper. We have made all of the changes that they have suggested as we believe that this has significantly improved the paper.

We address their comments in turn now.

Reviewer 1 (Rolf Sander).

"Section 5.2 provides a very interesting analysis of the ozone budget. Given the title of the manuscript, it is probably the most important section of all. Unfortunately, only two model runs are compared here. Additional model runs are not mentioned until section 6. I'd like to make the following suggestions:
[1] Present all model runs (including the sensitivity studies) in section 2, the model description section.
[2] For clarity, it may be helpful to define and use concise names instead of the somewhat lengthy phrases currently used for the sensitivity runs, e.g.: "no hal" ! "NOHAL" "standard GEOS-Chem (v9-2)" ! "BROMINE" "just iodine" ! "IODINE" "iodine simulation" ! "BR+I" or "FULLHAL"
[3] Add all simulations to Table A1, then move the table from the appendix into the main part.
[4] Add the results of NOHAL and IODINE to Table 7 and analyze their ozone budgets also in section 5.2."

[1] We attempted to include the description of all of the simulations (including the sensitivity studies) in together in a single section. This created a very long and turgid section which ended up destroying the flow of the paper and would present the reader with a somewhat confused perspective of our work. We would argue that the clarity of the paper in better with the current arrangement which described the iodine simulation against what is now the standard GEOS-Chem simulation (ie with bromine) (Sections 3, 4, 5). We then have a section where we compare the impacts of bromine and iodine (Section 6). We then have a section where we investigate the sensitivity of the iodine simulation to various uncertainties in the iodine chemistry (Section 7). We have adopted the reviewer suggestions on naming of the simulation and have tried to improve the clarity of the document.
[2] We have adopted this suggestion.
[3] We have adopted this suggestion
[4] We have adopted this suggestion.

"Abstract and elsewhere: "(350 < hPa < 900)"[.] This is incorrect. You probably wanted to write "(350 hPa < p < 900 hPa)" "
We have adopted this through the manuscript.

“The term OX is used in the abstract already but not defined until section 5.2. Please define all acronyms when they are first used. Other expressions that must be defined are: IOX, CH2IX, PAN, PMN, PPN, and MPN.“
We have updated to the text to include these definitions.

“ I think the introduction is much too long. For example, it contains [repetitions] like “The photolysis of O3 produces an electronically excited oxygen atom (O(1D)), which can react with a water molecule to produce two OH radicals.”
and “O3 is chemically lost in the troposphere predominantly through its photolysis in the presence of water to produce OH. ” I suggest to shorten the introduction significantly and simply refer to the review by Saiz-Lopez et al. (2012) in Chem. Rev.”
We have reduced the size of the introduction.

“It is difficult to judge the model output without knowing the model input, i.e. the distribution of the emission fields. The text only states that inorganic iodine emissions are calculated using equations from Carpenter et al. (2013). In accordance with the ACP data policy (http://www.atmospheric-chemistry-and-physics.net/about/data_policy.html), I suggest to provide the emission fields as a supplement to this article.”

A figures showing emission fields of inorganic iodine have now been added to the main section (Figure 1).

“ Page 20973, line 22: “. . . approximately evenly sources. . . ”
Something seems wrong with this sentence.”
We have updated the text.

“Page 20974, line 13: “lowest most model level”
Change to “lowermost”.”
We have updated the text.

“Section 5.2: Why are the numbers in the text different from the numbers in Tab. 7? The values are 748 vs 750 for iodine and 178 vs 184 for bromine.”
For iodine this was due to rounding issues and we have updated the text. For bromine this was a typo and we have updated the text.

“Page 20977: The calculation of the diurnal change is explained in the text as well as in the caption of Fig. 14. I don’t think it is necessary to duplicate this.”
We have removed the explanation from the text and just have it in the caption.

(2.09) Summary and Conclusion sections

“It is unusual to have two separate sections called “Summary” and “Conclusions”. Can they be combined?”

The summary (section 7.7) solely considers the information presented in the sensitivity section, whereas the conclusion section provides a plenary to the whole paper. We have changed the title to “Summary of sensitivity simulations” for clarity.

“Being a persistent publication, I’d prefer that you cite my paper (doi: 10.5194/acp-15-4399-2015) instead of my web page (Sander, 1999). The Henry’s law data in the paper and on the web are the same.”
The citation has been update to Sander et al (2015) as requested.

“In Table 2, you correctly list the physical Henry’s law constant of HI as 25 M/atm. However, the effective solubility, taking into account almost complete dissociation of HI into H+ and I-, is much larger. Is this considered in the model?”
We do consider the effective solubility. We have included text to explain this and updated the table.

“In Table 2, you give Vogt et al. (1999) as the reference for H(INO2) = 3:00 10-1 M/atm. However, Vogt et al. (1999) assume infinity. Please check this discrepancy.”
This was a mistake. The the Henry’s law for INO_2 given in table is by analogy with $BrNO_2$, not from vogt et al (1999). This has been updated in table 2.

“Table 3: I cannot see the reaction IO + ClO here. Is it not included in the mechanism?”
We do not consider chlorine chemistry in this version of the model. We have future plans to include chlorine chemistry.
(2.14) IO +_IO reaction

“Table 4: The reaction IO + IO [=>] I + OIO (T1) has no pressure dependence. Why is it listed as a termolecular reaction with “+O2” in the equation?”
Tables 3 and 4 have been updated to be clearer as to how we calculate termolecular reactions when pressure dependences are not available.

“Figure 6 and 7: You show the species IONO and IONO2 in the plots. They are probably the same as INO2 and INO3 in the text. A consistent terminology should be used.”
We have updated the text to be consistent.

“From the context, it becomes clear that Figures 7, 8, 9, 12, and 13 refer to the “iodine simulation”. Nevertheless, I think it would be helpful to mention this explicitly in the figure captions.”
The manuscript has been updated so that simulation name (e.g. “Br+I”) is included in all figure captions

“Fig. 14: The calculation of the diurnal change seems to be inconsistent. If you subtract the maximum ozone value, then you should also divide by the maximum (not the daily mean). For example, if the maximum is 100 nmol/mol, and the mean is 50 nmol/mol, then a complete (100 %) ozone destruction would result in

a diurnal change value of 200 % using your formula.”
We have changed out data processing to follow this suggestion and updated the figures and text. There is no change in our conclusions.

“According to the IUPAC Recommendations (page 1387 of Schwartz & Warneck “Units for use in atmospheric chemistry”, Pure & Appl. Chem., 67(8/9), 1377-1406, 1995, http://www.iupac.org/publications/pac/67/8/1377/pdf) the usage of “ppb” and “ppt” is discouraged for several reasons. Instead, “nmol/mol” and “pmol/mol” should be used for gas-phase mole fractions. I suggest to replace the obsolete units.”
“Page 20963, lines 22: “at high IO concentrations (> 2 pptv)”
Change to: IO mixing ratios.”

“Page 20977, lines 14: “BrO concentrations (0.4 pptv)”
Change to: BrO mixing ratios. ”
Units have been updated to recommended IUPAC units throughout the text and we have used mixing ratio instead of concentration.

Reviewer 2.

“This is a long manuscript and provides a lot of information. I would recommend to re-write some parts of this manuscript with clear organization. However, saying this - there is potentially some really good useful science here, it is just lost beneath the overload of figures and tables.”
Following both reviewer’s comments we have attempted to clarify the flow of the paper.

“Starting with the introduction section, 5 pages. It needs to be shortened. For example, the first paragraph could be a general explanation of the chemistry of the troposphere, including the main oxidants in the troposphere, OH and O3, and NO-NO2-O3 systems in the presence of organic compounds. The second paragraph, could start with the halogen chemistry and how it affects the ozone concentration.”
Both reviewers make this comment so we have shortened the introduction.

“Page 20962, line 28: Moreover, the recent sea-to-air flux climatology of Ziska et al. (2013) could be also cited in the global organic halogen emissions part.”
We have included this reference.

“I also agree with reviewer R. Sander that the model runs need to use concise names. Then section 2 and 6 would be clarified.”
We have adopted this suggestion.

“Section 2, page 20966, lines 15-16: The model is run for “two years, (2004-2006)” (this is three years!) and use “the final year 2005”? Something seems wrong with this part.”
This sentence has been updated to read “two years (2004 and 2005)” instead of “(2004-2006)”.

“I understand that in all the analysis, the model resolution is 2 x 2.5 and only the sensitivity studies are run with the model resolution at 4 x 5. I suggest to explain both model resolutions, 2 x 2.5 and 4 x 5, in section 2.”
We have included text to make this clear.

“In section 2.1 the parametrization for the inorganic iodine compounds from Carpenter et al. (2013) is briefly described. I suggest to briefly describe how these monthly emissions of Ordóñez et al. (2012) are calculated. For example, in the abstract of Ordóñez et al. (2012) “Ocean emissions of (...) parametrized by a biogenic chlorophyll a (chl-a) dependent source in the tropical oceans (...)“ ”
We updated the sentence on this within the text.

“In the last paragraph of section 3.1 is discussed the model overestimation of I2 concentrations. However, the parametrization for the inorganic iodine (I2, HOI) from Carpenter et al 2013 is not mentioned in this section. Could be any limitation in this parametrization that also contribute to the overestimation of I2? This parametrization depends on 1/wind speed. What happen at low wind speeds? I also agree with

reviewer R. Sander that the emission fields need to be included as a supplement to this article."
We have added a plot of the inorganic emissions to the paper (figure 1) and have indicated that the IX emissions ratio may also contribute to this in the text. We have updated the text to clarify the wind speed limits.

"Table 7 gives a lot of information, however only a few results are discussed in section 5.2. In addition, I couldn't find the global tropospheric OX loss of "184 Tg yr-1 from bromine chemistry" in Table 7. I suggest to rewrite this section in a clear way and thinking that the reader needs to find easily the information from Table 7 in Section 5.2."
We discuss key point in this table rather than going through all of the results which would become fairly turgid and boring. The table is designed to allow for a comprehensive comparison to other global model. We reviewer has noted a typo in our Ox loss for BrO which we have updated in the text.

(4.08) <u>Clarity of boxplots</u>

"Boxplots in the manuscript are confusing. For example lets take a look at Figure 4. From first glance its appears that the model and observations data are made at different latitudes or times stamps, and I assume this is not the case. The same for Figure 5 with the altitude. I suggest to plot both model and observations at the same time and latitude, instead of one next to the other, or explain in more detail what these boxplots show us."

"I suggest to give more information about the axis of each figure. Figures 5 and 11 miss the names of the species "IO" and "O3" in the x-axis. In addition, I suggest to use the same structure in the axis. For example in the axis of Fig. 4 " IO concentration (pptv)" and in the axis of Fig. 10 " O3 / ppbv"."
We have adopted the reviewer suggestions here and have attempted to improve the aesthetics of the plots as suggested and have included more information in the figure captions.

"Page 20960, second paragraph: I suggest to add after "to produce two OH radicals" that this process is dominated by the tropics."
This comment was considered with other reviewer comments when re-structuring the introduction, and broader description is now present within the introduction.

"Page 20966, line 3: Are there a lot of species that have linearized chemistry in the stratosphere as an upper BC for the troposphere? If there are only a few I suggest to specify these species."
In excess of thirty species are treated this way, therefore this have not been included within the text.

"Page 20966, line 19: "spun-up" Change to: spin-up"
Updated.

“Page 20967, Section 2.2: The last sentence in the first paragraph is repeated in the second paragraph.”

These two paragraphs describe wet and dry deposition respectively. The final sentence of each paragraph states the treatment of iodine aerosol in the model. The sentence has been amended to state whether it is referring to dry or wet deposition.

“Pages 20969-20970: Surface mixing [ratios] of IO, IO, OIO, HI, IONO and IONO2 from Figures 1 and 2 are not discussed in the document. It might be useful some discussion in sections 4.1 and 4.2.”

A Sentence has been added following the reviewers request. Due to limited or nonexistent measurements of these species in the remote marine boundary layer, these species offer limited ability to constrain the modelled values. Focus was given to comparing against the relative large, but still limited, dataset of observations IO in the literature.

“Page 20970, lines 13-14: “Concentrations of CH2ICl appear to be better simulated (Fig.3)”. We could say that CH2ICl is better simulated in the MBL. However, there is a lack of observational data above the MBL. A more detailed discussion is lacking here.”

The sentence describing CH2ICl observations has been updated from “Concentrations of CH2ICl appear to be better simulated (Fig 3)” to “Concentrations of CH2ICl appear to be better simulated in marine boundary layer where measurements are available (Fig 3).”

“Page 20970, line 22 : “over estimate” Change to: overestimate”

Updated.

“Page 20971, line 7: “over estimate”. Change to: overestimate”

Updated from “under and over estimates” to “under- and over- estimates”

“Page 20974, line 8: “tropspheric” Change to: tropospheric”

Updated.

“Page 20976, line 23: the word “O3” needs to be added after “Global tropospheric burdens of””

Updated.

“Page 20977, line 7: “fractional diurnal fractional”. Something seems wrong with this sentence.

The manuscript has been updated to remove the word repetition.

“Page 20980, first paragraph: The “I2Ox exp. X-sections” simulation is not defined in the manuscript.”

This was a typo and has been updated in the draft.

“Figure 11: The pressure needs to be turned in these plots. 1000 hPa should be in the surface and not in the top of the atmosphere.”
This had been updated.

Additional changes.

An additional IO observational dataset collected by coauthors (Rainer Volkamer, Ivan Ortega, and Roman Sinreich) was added to figure 5. This is in broad agreement with other datasets included and does not change the conclusions of the manuscript. Slight updates to the text have been made accordingly. Roman Sinreich and Ivan Ortega have been added to the author's list following this.

In addition, whilst reviewing the manuscript we noted the following errors:

In caption of figure 14 the text has been updated to correctly

from:

"Global annual mean surface O_3 loss (nmol/mol day^{-1}) from both bromine and iodine compared to a simulation with neither (top), comparison between modelled and observed fractional diurnal O_3 cycles at the Cape Verde Observatory for 4 simulations (bottom)."

to:

"Global annual mean surface O_3 loss (nmol/mol day^{-1}) in simulation "Br-I" from both bromine and iodine (top). Comparison between modelled and observed fractional diurnal O_3 cycles at the Cape Verde Observatory for "Br-I", "IODINE", "BROMINE" and "NOHAL" simulations (bottom)."

In table 7.

There was a transcription error in table 7, which has been updated. For other Ox sinks for the "Br-I" run the number shown was 173, when it should have been 179. This has been updated.

Manuscript prepared for Atmos. Chem. Phys. Discuss.
with version 2015/04/24 7.83 Copernicus papers of the LaTeX class copernicus.cls.
Date: 12 January 2016

Iodine's impact on tropospheric oxidants: a global model study in GEOS-Chem

T. Sherwen[1], **M. J. Evans**[1,2], **L. J. Carpenter**[1], **S. J. Andrews**[1], **R. T. Lidster**[1], **B. Dix**[3], **T. K. Koenig**[3,4], **R. Sinreich**[3], **I. Ortega**[3,4], **R. Volkamer**[3,4], **A. Saiz-Lopez**[5], **C. Prados-Roman**[5], **A. S. Mahajan**[6], **and C. Ordóñez**[7]

[1]Wolfson Atmospheric Chemistry Laboratories (WACL), Department of Chemistry,
University of York, York, YO10 5DD, UK
[2]National Centre for Atmospheric Science (NCAS), University of York, York, YO10 5DD, UK
[3]Department of Chemistry and Biochemistry, University of Colorado, Boulder,
CO 80309-0215, USA
[4]Cooperative Institute for Research in Environmental Sciences, University of Colorado, Boulder,
CO 80309-021, USA
[5]Department of Atmospheric Chemistry and Climate, Institute of Physical Chemistry Rocasolano,
CSIC, Madrid, 28006, Spain
[6]Indian Institute of Tropical Meteorology, Maharashtra, 411008, India
[7]Met Office, FitzRoy Road, Exeter, EX1 3PB, UK

Correspondence to: T. Sherwen (ts551@york.ac.uk)

Abstract

We present a global simulation of tropospheric iodine chemistry within the GEOS-Chem chemical transport model. This includes organic and inorganic iodine sources, standard gas-phase iodine chemistry and simplified higher iodine oxide (I_2O_X, ~~$X = 2, 3, 4$~~$_{X = 2, 3, 4}$) chemistry, photolysis, deposition and parametrised heterogeneous reactions. In comparisons with recent ~~Iodine Oxide~~ iodine oxide (IO) observations~~the iodine~~, the simulation shows an average bias of ~~$\sim +66$~~$\sim +90$ % with available surface observations in the marine boundary layer (outside of polar regions), and of $\sim +73$ % within the free troposphere (350 hPa ~~$<$ hPa $<$~~$< p <$ 900 hPa) over the eastern Pacific. Iodine emissions (3.8 Tg yr^{-1}) are overwhelmingly dominated by the inorganic ocean source, with 76 % of this emission from ~~Hypoiodous~~ hypoiodous acid (HOI). HOI is also found to be the dominant iodine species in terms of global tropospheric I_Y burden (contributing up to 70 %). The iodine chemistry leads to a significant global tropospheric O_3 burden decrease (9.0 %) compared to standard GEOS-Chem (v9-2). The iodine-driven O_X loss rate (see Footnote 1) (748 Tg O_X yr^{-1}) ~~is by~~ due to photolysis of HOI (78 %), photolysis of OIO (21 %), and reaction ~~of~~ between IO and BrO (1 %). Increases in global mean OH concentrations (1.8 %) by increased conversion of hydroperoxy radicals exceeds the decrease in OH primary production from the reduced O_3 concentration. We perform sensitivity studies on a range parameters and conclude that the simulation is sensitive to choices in parameterisation of heterogeneous uptake, ocean surface iodide, and I_2O_X (~~$X = 2, 3, 4$~~$_{X = 2, 3, 4}$) photolysis. The new iodine chemistry combines with previously implemented bromine chemistry to yield a total bromine and iodine driven tropospheric O_3 burden decrease of 14.4 % compared to a simulation without iodine and bromine chemistry in the model, and a small increase in OH (1.8 %). This is a significant impact and so halogen chemistry needs to be considered in both climate and air quality models.

1 Introduction

The chemistry of the troposphere controls the concentration of a range of climate gases including ozone (O_3) and methane (CH_4) (Kim et al., 2011; Voulgarakis et al., 2013; Young et al., 2013), and determines human and agriculture exposure to air quality pollutants such as O_3 and aerosols (Ainsworth et al., 2012; Fiore et al., 2012; Fowler et al., 2008). The chemical cycles maintaining concentrations of these atmospheric constituents are complex, and depend strongly upon the concentrations of O_3 and of the hydroxyl radical (OH) as key oxidants. Understanding the budgets and controls on these gases is therefore central to assessments of tropospheric chemistry (Voulgarakis et al., 2013).

The basic chemistry of O_3 and OH in the troposphere is coupled and the central aspects of this are well known (Young et al., 2013). ~~The photolysis of produces an electronically excited oxygen atom (), which can react with a water molecule to produce two OH radicals. Subsequent reaction of OH with organic compounds (hydrocarbons, oxygenates, methane, carbon monoxide etc.) produces peroxy radicals (R). If sufficient nitrogen oxide (NO) is available, the dominate fate of Rradicals is to oxidise NO to nitrogen dioxide (N), allowing the formation of via photolysis of . Tropospheric also has a source via transport from the stratosphere, and is lost to the Earth's surface via dry deposition.~~

Over the last decades significant research effort has gone into understanding the production of O_3, typically over continental regions due to its adverse impact on health and food security (Ainsworth et al., 2012; Fowler et al., 2008). However less emphasis has ~~been placed on its loss through~~ focussed on its chemical destruction. O_3 is chemically lost in the troposphere predominantly through ~~its~~ photolysis in the presence of water ~~to produce OH. Secondary sinks include reaction~~ or its reactions with HO_2 ~~or OH~~ and OH (Lelieveld and

---

[1] Here O_X is defined as $O_3 + NO_2 + 2NO_3 + PAN + PMN + PPN + HNO_4 + 3N_2O_5 + HNO_3 + BrO + HO$ where PAN = peroxyacetyl nitrate, PPN = peroxypropionyl nitrate, MPN = methyl peroxy nitrate, and MPN = peroxymethacryloyl nitrate.

Dentener, 2000). ~~Bromine~~ However, bromine and iodine compounds have also been identified as additional sinks for O_3 and as perturbations to OH cycling (Chameides and Davis, 1980; von Glasow et al., 2004). Of the two ~~compounds~~ iodine has arguably the more complex chemistry~~due to its many oxidation states, ability to form higher iodine oxides (, $X \geq 2$) and iodine particles . There are significant uncertainties in iodine chemistry kinetics, and a rapidly evolving body of knowledge on iodine sources which we now describe.~~ .

Historically the dominant source of iodine ~~in the atmosphere~~ was thought to be iodinated organic compounds from the ocean ~~. Initially methyl iodide () was considered the largest source but it was realised that even at the low observed concentration the very fast photolysis rates of other organo-halogens would lead to them playing a significant role~~ (Chuck et al., 2005; Jones et al., 2010; Law and Sturges, 2006). More recently, emission of inorganic halogen compounds (I_2 and HOI) has been identified as a ~~potentially significant flux of iodine into the atmosphere~~ significant source (Carpenter et al., 2013). ~~This mechanism was originally proposed by whereby uptake to the ocean and the subsequent reaction with Iodide () leads to volatilisation of inorganic iodine from the ocean. Based on laboratory studies, fluxes of HOI and have been parameterised as a function of surface iodide concentration, concentration, 10wind speed and surface temperature .~~

Our understanding of ~~the chemistry of iodine~~ its chemistry has been described in ~~detail in~~ recent publications (Saiz-Lopez et al., 2012b; Sommariva et al., 2012). Once emitted into the atmosphere, the highly labile iodinated precursors rapidly photolyse with lifetimes of seconds (e.g. I_2/HOI) to days (e.g. CH_3I) to release atomic iodine. The iodine can catalytically destroy O_3 by the reaction with of $O_3 + I$ to form IO, followed by secondary reactions ($+HO_2$, $+IO$, $+NO_2$, $+BrO$) which can regenerate atomic I without the abstracted oxygen. For instance IO reacts with HO_2, leading to HOI formation, and this is rapidly photolysed to reform I causing a net conversion of HO_2 to OH~~(Reaction **??**)~~.

~~A large body of experimental and theoretical work has been evaluated in JPL/IUPAC compilations . Whilst the key iodine reactions for processes of interest such as destruction (e.g. HOI, OIO photolysis) are now relatively well defined, the experimental rate data are limited or non-existent for certain processes. For example, ($X \geq 2$) photolysis~~

~~cross-sections and quantum yields, heterogeneous uptake parameters and the ultimate chemical fate are all poorly quantified, yet these reactions can significantly affect the lifetime. ($X \geq 2$)forms through combination reactions (R1)–(R5) however questions remain about their polymerisation, photolytic properties and eventual fate as discussed further by . Recent work has shown some of the key iodine species to be well buffered to mechanism uncertainties, but highlights the sensitivity of iodine concentrations and hence atmospheric impacts of this higher oxide chemistry~~ Much of the uncertainty in iodine chemistry involves the production and fate of their higher oxides (I_2O_X). These higher oxides are formed from a chain reaction of IO self reactions. (Sommariva et al., 2012).

$$O_3 + I \rightarrow IO + O_2 \tag{R1}$$

$$IO + IO \rightarrow OIO + I \tag{R2}$$

$$IO + IO \rightarrow I_2O_2 \tag{R3}$$

$$IO + OIO \rightarrow I_2O_3 \tag{R4}$$

$$OIO + OIO \rightarrow I_2O_4 \tag{R5}$$

Due to their short lifetimes and low ~~atmospheric~~ concentrations measuring iodine species poses significant challenges and so the observational dataset is sparse. For decades, measurements have focused on organic compounds and mainly CH_3I (Saiz-Lopez et al., 2012b). Technique development for in-situ measurements has led to an increase in data availability over the last decade, for both organic (e.g. CH_3I and CH_2IX, with $X = Cl$, Br, I) and inorganic (e.g. IO, OIO, I_2) species (Saiz-Lopez et al., 2012b). ~~Satellites may offer a mechanism to obtain global coverage, but retrievals at the low tropospheric concentrations are problematic .~~

Recent ~~organic and inorganic~~ measurements from aircraft (Dix et al., 2013; Volkamer et al., 2015; Wang et al., 2015), balloons (Butz et al., 2009), mountain tops (Puentedura et al., 2012), ground stations (Lawler et al., 2014; Mahajan et al., 2010; Read et al., 2008) and cruises (Großmann et al., 2013; Jones et al., 2010; Mahajan et al., 2012) ~~are establishing the global ubiquity of iodine compounds over the oceans. This increase in observations has~~ have enabled the development of global organic halogen emissions (Ordóñez et al., 2012; Ziska et al., 2013) and more recently, datasets of IO observations with extensive geographical coverage (Prados-Roman et al., 2015b; Volkamer et al., 2015; Wang et al., 2015).

~~Although the increase in coverage and type of observations has somewhat improved constraints of iodine compounds, the recently suggested inorganic ocean source (HOI) required to reproduce observed concentrations of IO remains unconstrained by in-situ direct flux observations. However, observations of marine boundary layer concentrations have been made recently . The inorganic emission requires knowledge of surface seawater iodide concentrations, but global iodide data remain spatially limited , and further complexities such as suppression of iodine emissions by dissolved organic matter also add uncertainty to the flux .~~

Iodine chemistry has been evaluated by a number of box model studies (Sander et al., 1997; Mahajan et al., 2009; McFiggans et al., 2000, 2010; Read et al., 2008; Saiz-Lopez et al., 2007) and a few global model studies (Prados-Roman et al., 2015a; Saiz-Lopez et al., 2012a, 2014). The initial focus was predominantly on geographic regions with elevated concentrations (e.g. polar Sander et al., 1997; Saiz-Lopez et al., 2007 and coastal Mahajan et al., 2009; McFiggans et al., 2000; Saiz-Lopez et al., 2006) and attempted to explain localised chemical perturbations mainly through the use of box models. ~~Iodine-driven loss was found to proceed through IO self reaction (Reactions **??–??**) at high IO concentrations (> 2),→ → → Net: → through (Reactions **??–??**) at lower IO concentrations ,→ + → → Net: → and by reactions between IO and BrO (Reactions **??–??**) where BrO concentrations are high.→ + → +→ → Net: →~~

When considered alongside bromine chemistry, box model studies have shown the magnitude of ~~these~~ halogen driven O_3 loss processes to be up to 45 % (Mahajan et al., 2009; Read et al., 2008) of the total loss. Iodine can change the local $HO_2 : OH$ ratio due to the production of HOI from HO_2 and IO~~(Reaction **??**)~~, and its subsequent photolysis to release OH ~~(Reaction **??**)~~ (Bloss, 2005; Chameides and Davis, 1980). Perturbation to the $NO : NO_2$ ratio has been shown to be significant at higher IO concentrations in polluted coastal locations (McFiggans et al., 2010) due to the ability of IO to oxidize NO into NO_2, which affects O_3 production. More recently, measurements in the marine boundary layer on ground-based island monitoring stations (Read et al., 2008; Mahajan et al., 2010; Gómez Martín et al., 2013), on ships (Großmann et al., 2013; Mahajan et al., 2010; Prados-Roman et al., 2015b), by balloon (Butz et al., 2009), and by aircraft (Dix et al., 2013; Volkamer et al., 2015; Wang et al., 2015) have demonstrated that these O_3 loss processes also occur in remote ~~locations (e. g. non-coastal). These studies highlight the vertical and global extent of iodine chemistry.~~ non-coastal locations.

Recently, the role of reactive halogens have also been investigated in global chemical transport models (Parrella et al., 2012) and chemistry-climate models (Ordóñez et al., 2012; Saiz-Lopez et al., 2014). ~~A study considering only bromine chemistry reported significant impacts on OH concentrations and burdens with decreases of 4 and 6.5, respectively . In a different study with a different model, inclusion of~~ Inclusion of tropospheric bromine, iodine and chlorine chemistry ~~led to topical tropospheric~~ into a global model led to significant changes in the composition troposphere. Tropospheric marine average O_3 columns ~~to~~ decrease on the order of ~~10~~$\sim$ 10 % (Saiz-Lopez et al., 2012a, 2014). As in the box model studies, up to $\sim$ 30 % of the O_3 loss in the marine boundary layer (900 ~~$<$ hPa~~hPa $<$p) is found to be driven by halogens (Saiz-Lopez et al., 2012a, 2014). Similarly, high levels of halogen-driven O_3 loss are also found in the upper troposphere (350 hPa ~~$>$ hPa $>$~~$>$ p $>$ ~~tropospause~~tropopause), with lower (10–15 %) impacts in the free troposphere (350 hPa ~~$<$ hPa $<$~~$<$ p $<$ 900 hPa) (Saiz-Lopez et al., 2012a, 2014).

In ~~this paper~~ order to explore our current understanding of the tropospheric chemistry of iodine we present a global modelling study of tropospheric iodine chemistry, using the GEOS-Chem chemical transport model. The new chemistry is described in Sect. 2. Section 3 describes the comparison of modelled iodine concentrations against observations. Then Sect. 4 describes modelled global chemical distributions by family. Impacts on O_3 and OH are described in Sect. 5. In Sect. 15 we consider interactions of iodine with bromine, and in Sect. 7 we look at key sensitivities of the simulation. Section 8 summarises our conclusions.

2 GEOS-Chem simulation

We use here the GEOS-Chem (http://www.geos-chem.org) chemical transport model version v9-02, with transport driven by assimilated meteorological and surface data fields (GEOS-5) from NASA's Global Modelling and Assimilation Office (GMAO). We have adapted the existing chemistry scheme which includes O_X, HO_X, NO_X, and VOC chemistry as described recently in Mao et al. (2013), bromine chemistry (Parrella et al., 2012), and a mass-based aerosol scheme. Stratospheric chemistry is climatologically represented based on LINOZ McLinden et al. (2000) for O_3 and linearised chemistry is applied for other species with concentrations taken from the Global Modelling Initiative (GMI) as described previously Murray et al. (2012).

Iodine tracers (I_2, HOI, IO, OIO, HI, INO_2, INO_3, I, INO, CH_3I, CH_2I_2, CH_2IBr, CH_2ICl, I_2O_2, I_2O_3, I_2O_4 and “aerosol iodine”) are included in the model. The modelled emissions, deposition, chemistry, photolysis and aerosol processes of these compounds are described below. No chemical processing of iodine species is performed in the stratosphere.

Notably our work differs from recent global iodine simulations (Saiz-Lopez et al., 2014) in its treatment of I_2O_X (~~$X = 2, 3, 4$~~$_X = 2, 3, 4$). Our ~~“standard iodine simulation”~~model (“Br+I”) considers the photolysis of these compounds whereas their “Base” simulation does not. This leads to our simulations having a more active iodine chemistry and this is discussed in 2.4.

As well as the core simulation present in this paper (“Br-I”), comparisons with the existing standard GEOS-Chem simulation (“BROMINE”) are presented which contain bromine chemistry as described in Section 2.6. When considering the coupling of iodine and bromine two additional simulations are include, one with just iodine chemistry (“IODINE”) and one with bromine or iodine chemistry (“NOHAL’).

For budgets and general analysis we run the model at 2° × 2.5° resolution for two years (~~2004–2006~~2004 and 2005) discarding the 1st “spin up” year and using the final year (2005) for analysis and budgets. For the sensitivity study (Section 7) the model is run with the same period for “spin up” and analysis, but at 4° × 5° resolution. The model output is discussed with focus on the marine boundary layer (900 ~~$<$ hPa~~hPa $<$p); the free troposphere (350 hPa ~~$<$ hPa $<$~~ $< p <$ 900 hPa); and upper troposphere (350 hPa ~~$>$ hPa $>$~~ $> p >$ tropopause). Comparisons with observations involve separate ~~spun-up~~ spin-up simulations, run with the date appropriate meteorology, sampled at the spatially and temporally nearest grid box and time step. We report here mixing ratios as pmol/mol or nmol/mol, which are equivilent to more widely used pptv/ppbv.

2.1 Iodine emissions

Both organic and inorganic iodine species (Table 1 and Figure 1) are emitted into the atmosphere. ~~Organic~~ Monthly emissions of organic iodine compounds (CH_3I, CH_2I_2, CH_2IBr, and CH_2ICl) are ~~emitted from the monthly emissions of~~ taken from Ordóñez et al. (2012) which parametrises fluxes based on chlorophyll a in the tropics and constant oceanic fluxes with 2.5 coast-to-ocean emission ratios for extratropical regions, and follows Bell et al. (2002) for CH_3I. Inorganic iodine compounds (HOI, I_2), formed from the uptake of O_3 to the ocean and the subsequent ocean surface reaction of O_3 with iodide (I^-), are emitted as calculated from Eqs. (19) and (20) in Carpenter et al. (2013). We parameterise ocean surface I^- concentration from the sea surface squared temperature relationship in Table 2 from Chance et al. (2014), the O_3 concentration in the ~~bottom-most~~ lowermost level of the model, and the 10 m wind speed from ~~metrological fields.~~ meteorological fields. The 10m wind speed used by the parameterisation is limited to a minimum of 5m/s to prevent unsubstantiated emissions at low wind speeds. Annual average iodine emission fluxes are shown in Figure 1.

Global emission totals (Table 1) are consistent with recent work (Saiz-Lopez et al., 2014) for organic iodine compounds as they also use Ordóñez et al. (2012). Inorganic fluxes calculated in this study are ~~32~~47 % ~~lower~~ higher than in previous work (Saiz-Lopez et al., 2014), despite using the same parameterisation (Carpenter et al., 2013; MacDonald et al., 2014). Although, model specific differences exist in sea surface temperatures, 10 m wind speeds and O_3 concentration the largest differences lie in the choice of parameterisation for sea surface iodide (see Sect. 7.5).

2.2 Iodine deposition

The model's deposition scheme has recently been updated (Amos et al., 2012). Dry deposition of the new iodine compounds is computed via the standard GEOS-Chem implementation of the "resistance-in-series" approach (Wesely, 1989) using literature Henry's law coefficients (Sander, 2015). This approach is applied to I_2, HI, HOI, INO_2, INO_3, I_2O_2, I_2O_3 and I_2O_4. Aerosol iodine is assumed to have the same wet deposition properties as sulfate aerosol.

Wet deposition is calculated for I_2, HI, HOI, INO_2, INO_3, I_2O_2, I_2O_3, and I_2O_4 for both large scale (frontal) and ~~convection~~ convective rain by applying scavenging in and below clouds (Liu et al., 2001) using species-specific values for Henry's law coefficients (Sander, 2015; Vogt et al., 1999) and molar heats of formation (Kaltsoyannis and Plane, 2008; Sander, 2015) as shown in Table 2. Fractionation between gas and liquid on ice is considered (Parrella et al., 2012; Stuart and Jacobson, 2003). Aerosol iodine is assumed to have the same dry deposition properties as sulfate aerosol.

2.3 Iodine chemistry scheme

The gas phase iodine chemistry is shown in Tables 3 and 4. We include all iodine reactions presented by recent IUPAC (Atkinson et al., 2007, 2008) and JPL 10-6 (Sander et al., 2011) compilations relevant to the troposphere. Some additional reactions are included based on recent work (Sommariva et al., 2012; von Glasow et al., 2002) as justified in Sect. A1.1. Reactions within aerosol following uptake of species (HI, HOI, INO_2, INO_3) and processing of higher iodine oxides (I_2O_X, ~~$X = 2,3,4$~~ $x = 2,3,4$) after formation of I_2O_X are not treated explicitly but are parameterised as described in Sect. 2.5.

2.4 Photolysis rates

Photolysis reactions are summarised in Table 5. Photolysis rates are calculated online using the standard FAST-J code implementation in GEOS-Chem (Mao et al., 2010). Cross-sections are processed to the 7 wavelength bins used by FAST-J (Bian and Prather, 2002). For most cross-sections JPL 10-6 (Sander et al., 2011) values were used. For I_2O_X ($X = 2,3,4$) we assume the same absorption cross section as INO_3, an approach used previously (Bloss et al., 2010). For most species (I_2, HOI, IO, OIO, INO, INO_2, I_2O_2, CH_3I, CH_2I_2, CH_2IBr and CH_2ICl) we assume a quantum yield of 1, but for INO_3 we use a quantum yield of 0.21 (Sander et al., 2011).

2.5 Heterogeneous processes

In line with previous studies (McFiggans et al., 2000), we consider that the uptake of HOI, INO_2 and INO_3 leads to the recycling of iodine back into the gas phase as $\frac{1}{2}$ I_2 on sea-salt aerosol alone, whereas irreversible loss via uptake of HI leads to the generation of aerosol phase iodine. Uptake of I_2O_X (~~$X = 2,3,4$~~$X = 2,3,4$) also leads to the generation of aerosol phase iodine (on any aerosol). Heterogeneous uptake rates are computed using the GEOS-Chem standard code (Jacob, 2000) from reactive uptake coefficients (γ). Reactions considered and values of γ used are based on recommendations and previous studies (see Table 6 and Sect. A1.2).

2.6 Model bromine ~~simulation~~chemistry

The bromine simulation in GEOS-Chem is described in Parrella et al. (2012) and this bromine chemistry is included in the ~~“standard simulation” throughout~~ simulations “BROMINE” and “Br-I” in the paper. Parrella et al. (2012) presented a range of comparisons against satellite BrO observations. Although in general the model reproduces many of the features, there is a systematic underestimation of tropospheric BrO. New aircraft observations show that tropospheric BrO (Volkamer et al., 2015; Wang et al., 2015) may be higher than within our simulation. Our simulation also underestimates surface BrO observed in the tropical Atlantic marine boundary layer (~~hPa <~~900 hPa $<$p) (~ 2 pmol/mol, Read et al., 2008) by a ratio of ~ 5 (0.4 pmol/mol). We consider the uncertainty in BrO concentration on our simulation as a part of our sensitivity study in Sect. 7.

3 Iodine model results and observation comparisons

In this section we describe and evaluate our iodine simulation ("Br+I"), which includes both iodine and bromine chemistry (Section 2.6). We initially focus on observational constraints for those iodine compounds that are directly emitted (Sect. 3.1), and then on the only secondary product which has been comprehensively observed (IO) (Sect. 3.2). We then turn to the averaged distribution of modelled iodinated compounds throughout the troposphere (Sect. 4).

3.1 Emitted iodine compounds

Figures 2 and 3 show annually averaged zonal (Fig. 2) and surface concentrations (Fig. 3) of organic and inorganic iodine precursors and their degradation products. These figures clearly illustrate the oceanic nature of iodine source species (CH_3I, CH_2I_2, CH_2ICl, CH_2IBr, HOI, I_2), with the highest concentrations over the tropical ocean. These plots also highlight the contribution of the included terrestrial CH_3I paddy field source (25 %) to global CH_3I concentrations from the Bell et al. (2002) emissions included in Ordóñez et al. (2012).

The emissions used here for organic iodine species have been assessed in (Ordóñez et al., 2012). We briefly present here a comparison between observations of CH_3I and CH_2ICl (Fig. 4) made during the UK Combined Airborne Studies in the Tropics (CAST) campaign over the tropical pacific (Guam) from January and February of 2014. These observations were made by gas chromatography mass spectrometry ~~(GC-MS)~~ as described in Andrews et al. (2015), using whole air samples from the Facility Airborne Atmospheric Measurement ~~(FAAM)~~ BAe 146-301 atmospheric research aircraft with techniques described in Andrews et al. (2013). The model shows an ability to capture the trend of decreasing concentration profile with height, but appears to underestimate the CH_3I concentrations (Fig. 4). Concentrations of CH_2ICl appear to be better simulated ~~(~~in marine boundary layer (900 hPa $<p$) where measurements are available (Fig. 4). Although not definitive, this brief comparison suggests the model, if anything, underestimates the concentration of organic iodine.

The first in-situ remote open ocean I_2 concentration measurements were made at Cape Verde (Lawler et al., 2014). This dataset reported concentrations increasing between dusk and dawn in the range 0.2 to 1.7 $\mathrm{pmol/mol}$ for the two separate measurement campaigns in May 2007 and May 2009 respectively. Our model captures the diurnal variation in I_2 of essentially zero during the day and increasing I_2 concentration during the night peaking just before dawn, but ranges between 2.5 and 7.5 $\mathrm{pmol/mol}$. Some component of this ~~over estimate~~ overestimate probably relates to the model's iodine heterogenous recycling which assumes 100 % conversion of HOI, INO_3, and INO_2 into $\frac{1}{2}$ I_2 rather than ICl and IBr which has been observed in laboratory studies (Braban et al., 2007).

3.2 Iodine oxide (IO) observations

Effectively, the only secondary iodine compound that has been observed and reported is IO. A comparison of a range of surface observations is shown in Fig. 5. Good agreement is seen in the West Pacific (TransBrom, Großmann et al., 2013) and tropical Atlantic at Cape Verde (Mahajan et al., 2010; Read et al., 2008), but the model has a generally high bias compared with other datasets (HALOCast-P, Mahajan et al., 2012; Malasapina, Prados-Roman et al., 2015b, TORERO ship Volkamer et al., 2015).

Biases between the daytime modelled and measured IO at Cape Verde and during the TransBrom cruise biases are within $\sim$ 22 and $\sim$ 16 % respectively. However, the model over-estimates the Malasapina cruise IO concentrations (bias $\sim +50$ to 250 %), ~~and both under and over~~ TORERO ship observations (bias +114 - 164 %), and both under- and over- estimates values from the HALOCast-P cruise (bias ~ -0.92 to 280 %). When all observations are latitudinally averaged (onto a 20° grid) a median bias of ~~66~~ $\sim +90$ % is found.

In Fig. 6 we show a comparison with recent aircraft IO observations from the TORERO aircraft campaign (Volkamer et al., 2015; Wang et al., 2015), which took place over the eastern Pacific. The model captures the vertical profile of IO but ~~over estimates~~ overestimates the observations (average bias of $+82$ % within the binned comparison). Biases in the comparison are greatest (bias = $+125$ %) in the marine boundary layer (~~hPa <~~900 hPa $<$p) and lowest (bias = $+73$ %) in the free troposphere (350 hPa ~~< hPa <~~ $< p <$ 900 hPa). The median bias in the upper troposphere (350 hPa ~~> hPa >~~ $> p >$ ~~tropospause~~tropopause) is $+95\,\%$.

From these comparisons it is evident that the model has some skill in simulating the average global surface distribution of IO (within a factor of 2) and similar skill at reproducing average vertical profiles. However, there is significant variability between locations, datasets and measurement groups. Increased global coverage, especially vertically, and inter-comparison of observational techniques are needed to better constrain the IO distribution.

4 Modelled distribution of iodinated compounds

We now analyse the modelled distribution of iodinated compounds. We start with the total gas phase inorganic iodine I_Y species ($2\mathrm{I}_2 + \mathrm{HOI} + \mathrm{IO} + \mathrm{OIO} + \mathrm{HI} + \mathrm{INO} + \mathrm{INO}_2 + \mathrm{INO}_3 + 2\mathrm{I}_2\mathrm{O}_2 + 2\mathrm{I}_2\mathrm{O}_3 + 2\mathrm{I}_2\mathrm{O}_4$) and then move to the distribution of the IO_X ($\mathrm{I} + \mathrm{IO}$) family.

4.1 Total inorganic iodine (I_Y)

The modelled iodine system is schematically shown in Fig. 7. Iodine emissions total $3.8\,\mathrm{Tg\,I\,yr^{-1}}$ with most of this ($3.2\,\mathrm{Tg\,I\,yr^{-1}}$) coming from the inorganic source (84 %). This is comparable to the 83 % calculated by Prados-Roman et al. (2015b) (Ocean only, 60° N–60° S). Most (56 %) of the emissions occur in the tropics (22° S to 22° N). Our emissions which include inorganic emissions, compare with reported values of $1.8\,\mathrm{Tg\,I\,yr^{-1}}$ (Saiz-Lopez et al., 2012a) and $2.6\,\mathrm{Tg\,I\,yr^{-1}}$ (Saiz-Lopez et al., 2014) which also include an inorganic source.

Previous studies that did not consider an inorganic iodine source give values of $0.58\,\mathrm{Tg\,I\,yr^{-1}}$ (Ordóñez et al., 2012), and $0.65\,\mathrm{Tg\,I\,yr^{-1}}$ (Jones et al., 2010), consistent with our organic emissions. HOI represents the single largest source of oceanic iodine (76 %) with averaged oceanic emissions of $1.4 \times 10^{8}\,\mathrm{atoms\,(I)\,cm^{-2}\,s^{-1}}$. This value is towards the lower end of flux values required to reproduce IO observations in recent box modelling studies (Großmann et al., 2013; Jones et al., 2010; Mahajan et al., 2009).

Annual mean surface concentrations (Fig. 3) of IO are ubiquitously found over the oceans at ($\sim 0.25-1$ pmol/mol). Minor species (e.g. HI, OIO) are modelled at greatest mixing ratios over the tropical oceans and towards the poles. Iodine compounds formed through interacts with NO_X (INO_3/INO_2) peaking in the northern hemisphere in polluted oceanic regions. However due to limited or non-existent measurements of these species in the remote marine boundary layer, these species offer limited ability to constrain the modelled values.

Iodine deposition is predominantly through HOI (51 %). The remainder is mostly through deposition of INO_3 (20 %) and aerosol iodine formed by heterogeneous loss of gaseous iodine (HI, I_2O_X) (24 %). The majority of the deposition sink is back into the ocean (91 %). The global I_Y lifetime is 3.3 days but where depositional scavenging is weakest (upper troposphere, 350 hPa ~~$>$ hPa $>$~~$>$ p $>$ ~~tropospause~~tropopause) this can increase by three orders of magnitudes.

Figures 8 and 9 show the average vertical and zonal distribution of iodine compounds through the troposphere. As expected given the surface source, the concentration of iodine drops with altitude. This drop is rapid across the top of the boundary layer. The concentrations of the short-lived source gases (CH_2IX (where X = Cl, Br, I) and I_2) are negligible outside of the lowest model levels but the concentrations of others (CH_3I and HOI) persist further through the column. For CH_3I this is due to its longer lifetime of ~ 4 days. However, the lifetime of HOI is ~~shorter~~ short (~ 4 min) and its persistence at higher altitudes reflects secondary chemical sources. From the top of the boundary layer to ~ 10 km the I_Y profile is flat due to the rapid convective mixing within the tropics, however above this mixing zone the concentrations decrease. The inorganic iodine within the tropical (22° N–22° S) upper troposphere (>10 km) is approximately equally sourced from upwards I_Y flux (6.6 Gg yr^{-1}) and organic iodine photolysis (7.9 Gg yr^{-1}), overwhelmingly of CH_3I. Overall, atmospheric iodine is dominated by three IOy species (HOI, IO, and INO_3) with HOI representing the greatest fraction (~ 70 %) in the free troposphere (350 hPa ~~$<$ hPa $<$~~$<$ p $<$ 900 hPa).

4.2 The iodine oxide family: IO_X (I + IO)

Globally IO_X production is dominated by inorganic iodine I_Y photolysis (HOI, 76 %; OIO, 11 %). The major loss route for IO_X is HOI production through IO reaction with HO_2 (~~Reaction ??,~~ 77 %), with additional loss routes through self-reaction, reaction with NO_X, and BrO contributing 10, 7.7, and 4.6 % respectively.

The global average IO_X lifetime with respect to chemical loss is ∼ 1 min, but increases within the tropical upper troposphere (350 hPa ~~$>$~~ $\geq p >$ ~~hPa $>$~~ tropopause) (up to 9 times) and beyond latitudes of 80° N and S (up to 4 times) due to colder temperatures. The major IO formation route (I + O_3) slows in these regions due to colder temperatures. This moves the partitioning of IO_X from IO to I. As the IO_X loss routes proceed predominantly through IO, the overall IO_X lifetime increases. This causes an increase in the annually averaged I to IO ratio which peaks with a ratio of 0.7–1.4 within the tropical upper troposphere (350 hPa ~~$>$~~ $\geq p >$ ~~hPa $>$~~ tropopause). This is at the lower end of the daytime range of 1–4 previously calculated (Saiz-Lopez et al., 2014). As described in Sect. 4.1, the I_Y (and thus the IO_X) in this region is approximately evenly ~~sources~~ sourced from photolysis of transported organic iodine species and direct transport of I_Y.

5 Impact of iodine on O_3 and OH

O_3 and OH are two key parameters for climate and air quality. Previous studies (Bloss et al., 2005; Saiz-Lopez et al., 2008, 2012a) have identified significant impacts of iodine on these compounds. Here we compare our model predictions to available observational constraints and then diagnose the model change.

5.1 Impact on O_3

On inclusion of iodine, the calculated global tropospheric O_3 burden drops from 367 to 334 Tg (9.0 %). Figure 10 shows the annual average ~~tropspheric~~ tropospheric column, surface and zonal change in O_3. On average the O_3 burdens in the marine boundary layer (900 ~~$<$ hPa~~hPa $<p$) decreased by 19.5 %, by 9.8 % the free troposphere (350 hPa ~~$<$ hPa $<$~~ $< p <$ 900 hPa), and 6.2 % in the upper troposphere (350 hPa ~~$>$ hPa $>$~~ $> p >$ ~~tropospause~~tropopause). The decrease is greater in the Southern Hemisphere (9.5 %), than the Northern Hemisphere (8.5 %).

Surface (~~lowest most~~ lowermost model level) O_3 shows an average decrease of 3.5 nmol/mol globally, with large spatial variability (Fig. 11) ~~and~~ with a greater decrease over the oceans (21 %) than the land (7.3 %). Comparing against the Global Atmospheric Watch (GAW, Sofen et al., 2015) surface O_3 observations (Fig. 11), there is no obvious decrease in the ability of the model to capture seasonality in surface O_3 although there is systematic decrease in O_3 concentration with the inclusion of iodine.

Figure 12 shows a comparison between a selection of annually averaged O_3 sonde profiles for the same year (2005, World Ozone and Ultraviolet Data Centre WOUDC, 2014) and our model simulation with and without iodine. A decrease in O_3 concentration is evident throughout the troposphere (average of 3.1 nmol/mol). As with comparison of surface observations (Fig. 12), no clear decline in model skill at capturing annual sonde profiles is apparent on inclusion of iodine, with some locations improving and others degrading. An exception to this is O_3 observations ~~greater than~~ south of 60° S at the surface where bias are increased and in the tropical free troposphere (350 hPa ~~$<$ hPa $<$~~ $< p <$ 900 hPa) where model O_3 biases are decreased.

5.2 O_3 budget

We diagnose the impact of iodine on O_3 by calculating the model's tropospheric odd oxygen budget in Table 7. Here we define O_X as defined in Footnote 1.

Iodine provides a global tropospheric O_X loss of ~~$\sim$ 750~~748 Tg yr^{-1} (15 % of the total). This is significantly larger than the ~~184~~178 Tg yr^{-1} from bromine chemistry and is comparable to the sink from the $O_3 + OH$ reaction. Overwhelmingly this loss is from the photolysis of HOI after its production from the reaction of IO with HO_2. The O_3 production term increases slightly ($\sim$ 1 %) with the inclusion of iodine reflecting small changes in the total reactive nitrogen ~~(N)~~ partitioning.

Iodine induced O_3 loss within the marine (land mask applied and between 50° N–50° S) troposphere of $\sim 540\,\mathrm{Tg\,yr^{-1}}$ is comparable to previous reported values Saiz-Lopez et al. (2014) when I_2O_X (~~$X = 2,3,4$~~$x = 2,3,4$) photolysis is included ($\sim 500\,\mathrm{Tg\,yr^{-1}}$).

Figure 13 shows the relative importance of different O_X sinks in the vertical. The “classical” O_3 loss routes ($h\nu + H_2O$, HO_X) dominate; however within the boundary layer and the upper troposphere (350 hPa ~~$>$ hPa $>$~~$> p >$ ~~tropospause~~tropopause), iodine represents 33 and 26 % of the total loss, respectively. The loss within the marine boundary layer (900 ~~$<$ hPa) in this study is again comparable to values reported recently of~~ hPa $<$p) is comparable to the 28 % reported in Prados-Roman et al. (2015a). This decreases rapidly with increasing altitude within the lower troposphere to values closer to 10 % reflecting the lower of IO concentrations (see Figs. 8 and 9). In the upper troposphere, higher IO_X and BrO_X concentrations lead to increased loss of O_3.

Figure 14 shows the zonal variation in the different O_X destruction terms (in terms of the O_X lifetime). It is evident that, in the model, iodine destruction is more spatially prevalent than bromine destruction, which is confined predominantly to the Southern Ocean. The impact of iodine is hemispherically asymmetric reflecting the higher NO_X in the Northern Hemisphere, higher BrO concentrations in the southern oceans and the larger ocean area in the Southern Hemisphere increasing emissions. Convective transport in the tropics rapidly lifts iodine species into the free troposphere (350 hPa ~~$<$ hPa $<$~~$< p <$ 900 hPa) where they can destroy O_3.

5.3 Impact on OH

Previous box model studies which investigated impact of iodine on OH concentration in the Antarctic (Saiz-Lopez et al., 2008), mid-latitude coastal (Bloss, 2005), tropical marine regions (Mahajan et al., 2010), and the free troposphere (Wang et al., 2015) found increases in the OH concentration due to IO enhancing conversion of HO_2 to OH. However we find that the inclusion of iodine in the model has little impact on the global mean OH concentrations ~~. It slightly increases~~ with it slightly increasing from 12.2 to 12.5×10^5 molecules cm^{-3}(1.8 %). This small increase is surprising given the 12 % reduction in the primary source ($O_3 + H_2O + h\nu$) due to lower O_3 concentrations. However, this is ~~to some extent,~~ more than compensated for by an increase in the rate of conversion of HO_2 to OH by IO. Previous studies using constrained box models (Bloss, 2005; Saiz-Lopez et al., 2008) could not consider this impact on the primary production of OH and it appears from our simulation that the overall impact is lower than previously thought.

6 Combined impact of bromine and iodine

The importance of halogen cross-over reactions ($BrO + IO$) for O_3 loss has been previously highlighted and found to be required to replicate observed diurnal surface O_3 loss in the marine boundary layer (Read et al., 2008). To explore these interactions a further two runs were performed~~:~~ , one simulation with iodine but without bromine (“~~just iodine~~IODINE”) and one without any halogens (“~~no hal~~NOHAL”).

~~Global~~ As shown in Table , the global tropospheric burdens of O_3 are 390, 367 (reduction of 5.9 %), 357 (8.5 %) and 334 Tg (14 %) for the simulations without halogens (“~~no ha~~NOHAL”), with just bromine (“~~standard simulation~~BROMINE”), with just iodine (“~~just iodine~~IODINE”), and with both iodine and bromine chemistry (“~~iodine simulation~~Br+I”) respectively. The sum of the changes in O_3 burden for the runs considering halogens individually is ~~very~~ slightly lower (0.1 %) than when considered simultaneously.

Figure 15 shows the combined daily surface loss rate of O_3 driven by bromine and iodine (upper panel). This correlates with IO concentrations (Fig. 3) reflecting iodine’s role in marine boundary layer O_3 destruction. Figure 15 also shows modelled and observed fractional diurnal fractional O_3 change at Cape Verde in the remote marine boundary layer (lower panel). ~~The diurnal change is calculated by subtracting each day’s maximum~~ For this comparison, observations (2006 to 2012, (Sofen et al., 2015)) and model data were first processed to average fractional diurnal change by averaging the values by hour of day, then subtracting the maximum average value of the diurnal. This fractional change was then divided by the average maximum value and multiplied by 100 to give % allow comparison between simulation runs with different O_3 ~~mixing ratio from hourly observations~~

~~(2006–2012,). Each value is then divided by the mean value for that day to give a fractional change , then this is presented averaged by hour over all the observations.~~ concentrations.

The simulation's fidelity increases significantly with the inclusion of iodine (Fig. 15) but there is little impact from bromine. Whereas modelled IO concentrations at Cape Verde shows agreement with observations (Fig. 5), BrO concentrations ($\sim 0.4\,\mathrm{pmol/mol}$) are significantly lower than reported ($\sim 2\,\mathrm{pmol/mol}$, Read et al., 2008). This underestimate of BrO in the model is a systemic problem (see Sect. 2.6) and so model estimates of the impact of Br on atmospheric composition described here are probably an underestimate.

Global mean tropospheric concentrations of OH are 12.80, 12.24, 13.02, and $12.47 \times 10^5\,\mathrm{molecules\,cm^{-3}}$ for the simulations without halogens ("~~no hal~~NOHAL"), with just bromine ("~~standard simulation~~BROMINE"), with just iodine ("~~just iodine~~IODINE"), and with both iodine and bromine chemistry ("~~iodine simulation~~Br+I") respectively. OH shows a differing response to bromine and iodine chemistry. As discussed in Sect. 5.3, inclusion of iodine leads to a small increase in OH concentrations. When solely iodine is considered, OH concentrations increase by 1.8 % compared to when no halogens are included. ~~Whereas bromine~~ Bromine chemistry leads to a reduction in OH (4.3 %), as reported previously (Parrella et al., 2012), due to enhanced production by HOBr photolysis not compensating for a decrease in the primary OH source ($O_3 + H_2O + h\nu$) from a reduced O_3 burden. The net impact overall on inclusion of halogens is a global reduction in OH (2.6 %).

In our simulations, the global impact of Br and I chemistry are essentially additive with apparently limited impact from the cross reactions. The global impact of iodine appears significantly larger than that of bromine, however, given that the model underestimates the concentrations of Br compounds this should be subject to future study.

7 Sensitivity studies

As discussed in the introduction, a range of uncertainties exist in our understanding of tropospheric iodine. We perform sensitivity analysis on some of these parameters using the 4° × 5° version of the model. We chose to analyse the sensitivity to inclusion of inorganic iodine emissions, heterogeneous loss and cycling, photolysis rates and ocean surface iodide. Values are quoted as a % change from the ~~iodine~~ “Br+I” simulation described in Sects. 2–5. Figure 17 summarises the fractional impact of these experiments on the globally averaged vertical distribution of I_Y, O_3 and vertical profile comparison of observations of IO from the TORERO aircraft campaign (Volkamer et al., 2015; Wang et al., 2015). Additional information is listed in Table A1 in the Appendix A.

7.1 Just Organic Iodine

Until recently many studies solely considered organic iodine (Jones et al., 2010; Ordóñez et al., 2012) emissions. As discussed in Sect. 3.1, our simulation uses the Carpenter et al. (2013) inorganic emission parameterisation as well as organic iodine emissions from Ordóñez et al. (2012). When we just consider organic iodine emissions (“Just org. I”) we find that global I_Y burdens decrease (~~$\sim$ 65~~65 %), and mean surface marine boundary layer (900 ~~$<$ hPa~~hPa $<$p) IO decreases (~~$\sim$ 83~~83 %). The median bias against TORERO aircraft IO observations decreases by ~~$\sim$ 68~~68 % ~~and becomes~~ to become a negative bias of −25 %. The decreased I_Y leads to the mean global OH decreasing by 0.64 % and global tropospheric O_3 increasing by 5.5 %.

7.2 Heterogeneous uptake and cycling

There is limited experimental data for the reaction probability (γ) for iodine species on aerosol. Our base case scheme follows the literature precedent (McFiggans et al., 2000) and assumes a heterogeneous recycling of unity (e.g. ~~HOI=$\frac{1}{2}$~~HOI $\rightarrow \frac{1}{2}I_2$) on sea salt which is not limited by aerosol acidity. However, the acidity of aerosol may limit iodine cycling as not all sea-salt aerosols are acidic (Alexander, 2005) and other aerosols may irreversibly uptake iodine. Detail on the ~~reaction probabilities (γ)~~ chosen is in Appendix A (Section A1.2). To explore these uncertainties four simulations were run: (1) with the γ values that ~~led~~ lead to I_2 release doubled (“het. cycle ×2”), (2) with the γ values halved (“het. cycle /2”), (3) with all uptake reactions leading to a net loss of iodine (“No het. cycle”), and (4) a run where sulfate aerosol leads to a sink for iodine with the same γ values as for sea salt (“Sulfate uptake”).

Increasing the heterogeneous cycling (“het. cycle $\times$2”) converts more HOI (the dominant I_Y species) into I_2, thus reducing the rate of HOI deposition. The global I_Y burden increases by ~~$\sim$ 6~~6 %, mean surface marine boundary layer (900 ~~$<$ hPa~~hPa $<$ p) IO concentration increases by ~~$\sim$ 2~~2 % and the median bias with respect to the TORERO aircraft IO observations increases by ~~$\sim$ 26~~ 26 to 100 % (Fig. 17). Decreasing the heterogeneous cycling (“het. cycle /2”) has the opposite impact of roughly the same magnitude~~. Global~~, global average I_Y burden decreases (~~$\sim$ 4.3~~4.3 %), average surface marine boundary layer IO decreases (~~$\sim$ 1.8~~1.8 %) and the median bias with respect to the TORERO aircraft IO observations decreases (~~$\sim$ 18~~18 %) to 66 %.

The impacts of theses changes is small overall. Increased iodine cycling leads to a decrease in the tropospheric O_3 burden of ~~$\sim$ 0.69~~0.69 % and global mean OH increases by ~~$\sim$ 0.05~~0.05 %, whereas decreased cycling leads to the tropospheric O_3 burden increasing by ~~$\sim$ 0.56~~0.56 % and OH decreasing by ~~$\sim$ 0.09~~0.09 %.

By removing the release of I_2 to the gas-phase following uptake of iodine (“no het. cycle”) or by considering irreversible iodine loss to sulfate aerosol (“Sulfate uptake”) the global I_Y burdens decrease significantly by 47 and 48 %, respectively. Surface marine boundary layer (900 ~~$<$ hPa~~hPa $<$ p) IO concentration decreases by 48 and 22 %. The median bias with respect to the TORERO aircraft IO observations decreases in the case of “no het. cycle” (~~$\sim$ 84~~84 %) to 13 % and decreases in “Sulfate uptake” (~~$\sim$ 92~~92 %) to -6.7 %. The “Sulfate uptake” scenario shifts the median bias with the TORERO aircraft IO observations to be negative, instead of positive (~~$\sim$ +80~~+80 % for ~~the base iodine simulation at 4 $\times$ 5~~“Br+I” at 4° × 5°).

This large decrease in I_Y ~~decreases~~ reduces the potency of iodine chemistry. The reductions in the tropospheric O_3 burdens (4.1 and 4.5 % for “no het. cycle” and “Sulfate uptake”) are comparable to the simulation where only organic iodine sources are considered (5.5 %, “Just I Org.”). Global mean OH decreases slightly by ~~$\sim$ 0.54 and $\sim$ 0.87~~0.54 and 0.87 %

under these two scenarios. These two sensitivity runs represent large perturbations to the iodine system, highlighting the importance and uncertainties in heterogeneous chemistry.

7.3 Uncertainties in photolysis parameters

Absorption cross-sections and quantum yields for iodine species are few and their temperature dependencies are not known. Notably, the absorption cross sections for the higher iodine oxides (I_2O_2, I_2O_3, I_2O_4) are highly uncertain (Bloss et al., 2001; Gómez Martín et al., 2005; Spietz et al., 2005) and we use the INO_3 spectrum in our simulation. This uncertainty was tested in 3 simulations: (1) absorption cross-sections were doubled (“I_2O_X X-sections ×2”), (2) tentative literature assignments of spectra were used for I_2O_3 and I_2O_2 (Bloss et al., 2001; Gómez Martín et al., 2005; Spietz et al., 2005), with I_2O_2 used for I_2O_4 (“I_2O_X exp. X-sections”), (3) and finally no I_2O_X photolysis at all was considered (“No I_2O_X photolysis”).

Sensitivity runs “I_2O_X X-sections ×2” and “I_2O_X exp. X-sections” increase photolysis rates, therefore resulting in an increase in the I_Y lifetime of 5.3 and 8.3 % and the I_Y burdens by 3.1 and 4.8 % respectively. The average surface marine boundary layer (900 ~~$<$ hPa~~hPa$<$p) IO concentration responds by increasing by 4.3 and 6.7 % for “I_2O_X X-sections ×2” and “I_2O_X exp. X-sections” respectively. Both these simulation increase median bias with TORERO aircraft IO observations by ~~$\sim$ 4.8~~ 4.8 to 84 % and ~~$\sim$ 7.6~~ 7.6 to 86 %, respectively. The impacts on O_3 burden are small with a decrease of 0.4 and 0.6 % for “I_2O_X X-sections ×2” and “I_2O_X exp. X-sections” respectively. Global mean OH concentrations increase by 0.05 and 0.09 % respectively.

The removal of I_2O_X (~~$X = 2,3,4$~~$X = 2,3,4$) photolysis reduces the global tropospheric I_Y burden (~~$\sim$ 35~~35 %), reduces surface marine boundary layer (900 ~~$<$ hPa~~hPa$<$p) IO (~~$\sim$ 40~~40 %), increases tropospheric O_3 burden (5.1 %) and decreases global mean OH (0.9 %) with respect to ~~the base iodine simulation~~“Br+I”. The median bias with respect to the TORERO aircraft IO observations becomes negative and decreases by ~~$\sim$ 81~~ 81 to -16 %, illustrating a large change in the simulated IO profile by removing the I_2O_X photolysis

(Fig. 17). This was also noted by Prados-Roman et al. (2015b) with respect to surface observations.

Our “No I_2O_X photolysis” simulation is akin to the “base” simulation of (Saiz-Lopez et al., 2014). This was presented as a lower bounds for iodine chemistry. Their “JI_XO_Y” simulation, is akin to our ~~iodine simulation~~“Br+I”. Saiz-Lopez et al. (2014) find a decrease in marine tropospheric O_3 column burden of 3.0 and 6.1 % compared to a simulation with no iodine chemistry for their “base” and “JI_XO_Y” simulations respectively. Considering the same domain our comparable simulations show values of 4.0 to 8.7 %.

7.4 Marine boundary layer BrO concentration

As discussed in the introduction and Sect. 15, bromine and iodine chemistry are potentially coupled. GEOS-Chem ~~appears to underestimate~~ underestimates BrO (Parrella et al., 2012), with for example, our simulation underestimating the BrO concentrations at Cape Verde (Read et al., 2008) (~ 2 pmol/mol) by a factor of ~~∼ 5.~~ around 5.

To test the sensitivity of the model to BrO concentrations, a simulation with BrO concentration fixed at 2 pmol/mol in the daytime marine boundary layer was run (“MBL BrO 2 pmol/mol”). Increased BrO leads to increased OIO concentrations ($BrO + IO \rightarrow OIO + Br$~~, ??~~), which leads to increased higher oxide production which in turn increases I_Y loss and decreases I_Y burden (10 %). The median bias in vertical comparisons with TORERO aircraft IO observations decreases by ~~∼ 12~~ 12 to 71 %. Although the overall tropospheric O_3 burden decreases by 3.7 %, the average O_3 change at the surface is larger and shows a decrease of ~~∼ 8~~88 % (Fig. 17) which is the largest decrease in O_3 found within these sensitivity simulations.

7.5 Ocean surface iodide (I^-) concentration

Chance et al. (2014) compiled the available ocean surface iodide (I^-) observations and investigated correlations with various environmental parameters. They found that ocean surface iodide correlated most strongly with the square of sea surface temperature, as used in this work. However MacDonald et al. (2014), using a sub-set of the Chance et al. (2014) data, found that an Arrhenius parameterisation gave best agreement. Figure 16 shows annual averaged ocean surface iodide generated from both parameterisations. The sea surface temperatures are taken from the annual mean GEOS field used in GEOS-Chem. The area weighted mean concentrations are 37.6 and 80.8 nM for MacDonald et al. (2014) and Chance et al. (2014), respectively. Both approaches reproduce the latitudinal gradient observed in Fig. 1 of Chance et al. (2014), however large ~~discrepancies are~~ differences apparent in magnitude. The dataset reported in Chance et al. (2014) has a median value of 77 nM and interquartile range of 28–140 nM.

Inclusion of the MacDonald et al. (2014) iodide parameterisation (“Ocean Iodide”) reduces the inorganic iodine flux by 51 % to 1.9 Tg, which in turn decreases the global tropospheric iodine I_Y burden (23 %) and surface IO concentrations (34 %). The median bias in comparison with TORERO vertical profiles decreases by ~~$\sim$ 47~~ 47 to 42 %. Tropospheric O_3 burden increases by 2.1 % and global mean OH increase by 0.17 % with respect to ~~the iodine simulation~~“Br+I”.

7.6 Higher oxide lifetime

Within the model we have considered the uptake of the I_2O_X (~~$X = 2,3,4$~~$_{X=2,3,4}$) to aerosol as an irreversible loss of iodine, with the same reactive probability (γ) as INO_2 (0.02). We assess our sensitivity to this assumption by running simulations doubling (“I_2O_X (γ) $\times 2$”) and halving this value (“I_2O_X $(\gamma)/2$”).

The effect of doubling γ leads to decreasing global tropospheric I_Y burden (5.1 %), decreasing surface marine boundary layer (900 ~~$<$ hPa~~hPa$<$p) IO (4.6 %), and decreases the median bias in vertical comparisons with TORERO ~~IO ($\sim$ 6.9~~aircraft IO (6.9 %) to 75 %. This leads to a slightly increased global tropospheric O_3 burden (0.54 %), and marginally decrease in global mean OH (0.08 %). The effect of halving γ is essentially symmetrical, with an increased global tropospheric I_Y burden (4.3 %), increased surface marine boundary layer (900 ~~$<$ hPa~~hPa$<$p) IO concentration (4.3 %), and an increased median bias in vertical comparisons with TORERO ~~IO by $\sim$ 4.4~~ aircraft IO by 4.4 to 84 %. This leads to slightly decreased global tropospheric O_3 burden (0.44 %), and marginally increase in OH (0.05 %).

7.7 Summary of sensitivity simulations

Uncertainties in the atmospheric chemistry of iodine lead to some significant uncertainties on iodine’s impact ~~of~~ on atmospheric composition. Further laboratory studies on the photolytic properties of high oxides would reduce uncertainty, as would a more detailed understanding of the rates of heterogenous cycling on a range of aerosols. The interplay between bromine and iodine chemistry is also potentially significant for the oxidant budgets. Given the inorganic iodine ~~emission’ s~~ emissions’ role as the largest source of iodine into the atmosphere, improved constraints on the concentration of oceanic iodide would also reduce uncertainties. It is clear that we do not have a complete understanding of iodine chemistry in the atmosphere and further laboratory and field observations are necessary to provide a stronger constraint.

8 Conclusions

We have implemented a representation of the tropospheric chemistry of iodine into the GEOS-Chem model and compared it against a range of observational datasets. We estimate a global emission of 3.8 $\mathrm{Tg\,yr^{-1}}$ of iodine, which is consistent with previous work. We find this dominated by the inorganic ocean source (84 %), and the majority (91 %) of deposition is back to the oceans.

Comparisons with the limited IO observational dataset shows that the model is within a factor of 2 of the observations on average. Iodine reduces the global tropospheric O_3 burden by ~~~ 9~~ ~ 9 %. Global mean OH concentrations are increased (1.8 %) by the presence of iodine due to the reduction in the O_3-H_2O primary source being compensated for by an increased conversion of HO_2 into OH via the photolysis of HOI. Both changes involve HOI production and destruction cycles.

Our understanding of iodine chemistry is hampered by limited laboratory studies of both its gas and aerosol phase chemistry, by limited field measurements of atmospheric iodine compounds and poor understanding of ocean surface iodide and its chemistry. Impacts on O_3 and OH are sensitive to the uncertainty of ocean iodine emissions, the parameterisation of iodine recycling in aerosol, to the photolysis parameters for the higher oxides and to the assumed Br chemistry. Given its role as the largest component of atmospheric iodine, and its central role in both O_3 destruction and HO_2 to IO cycling, a priority should be given to instrumentation to measure HOI.

Appendix A:

A1 Additional details on sensitivity runs

A1.1 Details of reactions within scheme, but not present within IUPAC/JPL

The field of iodine chemistry is still young, and some reactions that are used within box model/global studies are not in the IUPAC/JPL compilations due to uncertainties in the laboratory studies or for other reasons. Differences choices have been made regarding reactions included in previous box model (Bloss et al., 2010; Mahajan et al., 2009; Read et al., 2008; Saiz-Lopez et al., 2008; Sommariva et al., 2012) and global model studies (Breider, 2010; Ordóñez et al., 2012; Saiz-Lopez et al., 2012b, 2014). The following reactions have been included within our simulation's chemistry scheme (Tables 3 and 4) although they are not in the IUPAC/JPL compilations.

$$\mathrm{M5{-}HOI + OH \rightarrow IO + H_2O}$$

Uncertainties exist over product channels for this reaction (Sommariva et al., 2012). In our study we assume the products are IO and H_2O based on laboratory experiments (Riffault et al., 2005) and previous box model analysis (Sommariva et al., 2012). ~~It is not included~~

~~within JPL/IUPAC compilations.~~

$M12-INO_3 + I \rightarrow I_2 + NO_3$

This reaction's rate is based on a single theoretical study (Kaltsoyannis and Plane, 2008)~~, and it is thus not included within either the JPL or IUPAC compilations~~. The impact of inclusion within a box model was found to be minimal, except in high iodine and NOx conditions (Sommariva et al., 2012). ~~It is argued that this reaction rate needs determination with higher accuracy .~~

$M17-OIO + OIO \rightarrow I_2O_4$

This reaction rate is from a single experimental study (Gómez Martín et al., 2007), which yielded a lower limit ~~at~~ of $1.2\pm0.3\times10^{-10}$ cm^3 molecules^{-1} s^{-1}. This reaction is ~~not included within JPL/IUPAC compilations. This reaction is included~~ included in this work, along with the reverse reaction (Reaction ~~T12~~M24, $I_2O_4 \rightarrow 2OIO$).

$M26-INO_3 \xrightarrow{M} IO + NO_2$

~~Good consensus exists between reaction rates (298) for the forward reaction (Reaction T7) from JPL (7.68×10^{-31}) and IUPAC (7.96×10^{-31}). The reverse reaction (Reaction T8)~~ The reaction is included in the IUPAC (Atkinson et al., 2007) without direct experiment observation. No recommendation is given in the recent ~~recent~~ JPL compilation (Sander et al., 2011). The INO_3 thermal stability used by studies has led ~~to magnitude of differences~~ significant range between reaction rates (298 K) from 1.08×10^{-2} (Read et al., 2008) to 2.51×10^{-5} cm^3 molecules^{-1} s^{-1} (Sommariva et al., 2012). The latter uses the most recent theoretical study (Kaltsoyannis and Plane, 2008), which we also use here. The forward reaction (Reaction ~~T7~~M25) has been included ubiquitously in iodine modelling work; and reverse reaction (Reaction ~~T8~~M26) is employed in the majority of, but not all studies (Ordóñez et al., 2012). Both reactions are included in this work.

$M21-IO + OIO \xrightarrow{M} I_2O_3$

A single experimental study (Gómez Martín et al., 2007) gives a upper limit and lower rate limit of 1.5×10^{-10} and $1.5 \times 10^{-11}\,\mathrm{cm^3\,molecules^{-1}\,s^{-1}}$, respectively. We use the higher value in this work as in others studies (Saiz-Lopez et al., 2008; Sommariva et al., 2012). ~~The rate was found to increase with pressure over the range studied (10–400,), suggesting greater importance at the higher pressures found at the surface.~~

$$\mathrm{M22{-}I_2O_2 \xrightarrow{M} IO + IO}$$

$$\mathrm{M23{-}I_2O_2 \xrightarrow{M} OIO + I}$$

These reaction has been studied solely theoretically (Kaltsoyannis and Plane, 2008)~~and are not included in JPL/IUPAC compilations~~. A temperature dependent rate was calculated theoretically ~~using the Rice–Ramsperger–Kassel–Markus theory~~ (Ordóñez et al., 2012) which is used in our work.

$$\mathrm{M24{-}I_2O_4 \xrightarrow{M} 2OIO}$$

The rate is calculated from the value for binding energy of the dimer (Kaltsoyannis and Plane, 2008)~~, and is not included in JPL/IUPAC complications. Considering that we~~ . As have included reaction M17 ($\mathrm{OIO + OIO \rightarrow I_2O_4}$), we also include the reverse Reaction ~~T12~~ M24 in our work at the Kaltsoyannis and Plane (2008) rate.

A1.2 Detail of reactive uptake coefficients (γ) used for heterogeneous reactions

As described in Sect. 3.1, we stoichiometrically emit I_2 following uptake of species that hydrolyse to HOI (INO_2, INO_3, HOI). We assume this to avoid double counting of Br release already included within the model as described by Parrella et al. (2012). Lack of, or limited experimental data reduces certainty on heterogeneous processing of halogens. The reactive uptake coefficients (γ) used in this study are experimentally constrained wherever possible or follow previously estimated values in the literature as described below.

The JPL compilation notes a single experimental study of HOI uptake on H_2SO_4, yielding mass accommodation coefficients (α) in the range 0.02 to 0.07 (Sander et al., 2011).

Another two studies on ice and salt are reported in JPL ~~10-6~~ with lower limits of ~~> 0.0022 and > 0.01~~ 0.0022 and 0.01 respectively (Sander et al., 2011). IUPAC evaluates two experimental studies which “concur (the) uptake coefficient is large”, but no recommendation is given due to possible uncertainties in reversibility (Crowley et al., 2010). The γ values used in literature range between 0.01 (Mahajan et al., 2009; Breider, 2010) and 0.5 (Saiz-Lopez et al., 2007). The higher end of this range originates from an investigation of the sensitivity to this a parameter ~~within THAMO~~ by Saiz-Lopez et al. (2007) for which the basecase was set as 0.02. A γ value of 0.02 is used within our work.

For INO_2 and INO_3 no experiment work is available on the uptake and values have previously been estimated by analogy with measured equivalent bromine species. For INO_3 a γ value of 0.01 has been frequently used based on estimations (Mahajan et al., 2009; Ordóñez et al., 2012), but values have been used up to 0.2 (Bloss et al., 2010). For INO_2 γ values of 0.01 (Mahajan et al., 2009) or 0.02 (Ordóñez et al., 2012; Saiz-Lopez et al., 2007) have often been used, but γ values up to 0.1 have also been used (Bloss et al., 2010). In this work γ values of 0.01 and 0.02 are used for INO_3 and INO_2 respectively.

The IUPAC compilation includes a recommendation for HI uptake γ on ice of 0.2 (Crowley et al., 2010), based on three experimental studies. A γ value of 0.1 though has most often been used in modelling studies (Breider, 2010; Mahajan et al., 2009; Saiz-Lopez et al., 2008) and is ~~is~~ used in this work.

For I_2O_X (~~$X = 2,3,4$~~ $x = 2,3,4$) no experimental data is available for reactive uptake coefficients. The uptake has been discussed in the literature, including a box model study which tested sensitivity around a base value of 0.02 (Saiz-Lopez et al., 2008). The γ value for I_2O_X was set at 0.02 by with analogy INO_2. This value is highly uncertain and values up to 1 have been used for gamma in modelling studies (Bloss et al., 2010). A value of 0.02 is used within this work.

Acknowledgements. This work was funded by NERC quota studentship NE/K500987/1 with support from the NERC BACCHUS and CAST projects NE/L01291X/1, NE/J006165/1.

R. Volkamer acknowledges funding from US National Science Foundation CAREER award ATM-0847793, AGS-1104104, and AGS-1452317. The involvement of the NSF-sponsored Lower Atmospheric Observing Facilities, managed and operated by the National Center for Atmospheric Research (NCAR) Earth Observing Laboratory (EOL), is acknowledged.

T. Sherwen would like to acknowledge constructive comments from and conversations with all coauthors as well as R. Chance and J. Schmidt.

~~This work was funded by NERC quota studentship NE/K500987/1 with support from the NERC BACCHUS and CAST projects NE/L01291X/1, NE/J006165/1.~~

References

Ainsworth, E. A., Yendrek, C. R., Sitch, S., Collins, W. J., and Emberson, L. D.: The effects of tropospheric ozone on net primary productivity and implications for climate change, Annu. Rev. Plant Bio., 63, 637–661, doi:10.1146/annurev-arplant-042110-103829, 2012.

Alexander, B.: Sulfate formation in sea-salt aerosols: Constraints from oxygen isotopes, J. Geophys. Res., 110, D10307, doi:10.1029/2004JD005659, 2005.

Amos, H. M., Jacob, D. J., Holmes, C. D., Fisher, J. A., Wang, Q., Yantosca, R. M., Corbitt, E. S., Galarneau, E., Rutter, A. P., Gustin, M. S., Steffen, A., Schauer, J. J., Graydon, J. A., Louis, V. L. St., Talbot, R. W., Edgerton, E. S., Zhang, Y., and Sunderland, E. M.: Gas-particle partitioning of atmospheric Hg(II) and its effect on global mercury deposition, Atmos. Chem. Phys., 12, 591–603, doi:10.5194/acp-12-591-2012, 2012.

Andrews, S. J., Jones, C. E., and Carpenter, L. J.: Aircraft measurements of very short-lived halocarbons over the tropical Atlantic Ocean, Geophys. Res. Lett., 40, 1005–1010, doi:10.1002/grl.50141, 2013.

Andrews, S. J., Hackenberg, S. C., and Carpenter, L. J.: Technical Note: A fully automated purge and trap GC-MS system for quantification of volatile organic compound (VOC) fluxes between the ocean and atmosphere, Ocean Sci., 11, 313–321, doi:10.5194/os-11-313-2015, 2015.

Atkinson, R.: Atmospheric chemistry of VOCs and NO_x, Atmos. Environ., 34, 2063–2101, doi:10.1016/S1352-2310(99)00460-4, 2000.

Atkinson, R., Baulch, D. L., Cox, R. A., Hampson, R. F., Kerr, J. A., Rossi, M. J., and Troe, J.: Evaluated kinetic and photochemical data for atmospheric chemistry: Supplement VIII, halogen species – IUPAC Subcommittee on gas kinetic data evaluation for atmospheric chemistry, J. Phys. Chem. Ref. Data, 29, 167–266, doi:10.1063/1.556058, 2000.

Atkinson, R., Baulch, D. L., Cox, R. A., Crowley, J. N., Hampson, R. F., Hynes, R. G., Jenkin, M. E., Rossi, M. J., and Troe, J.: Evaluated kinetic and photochemical data for atmospheric chemistry: Volume III – gas phase reactions of inorganic halogens, Atmos. Chem. Phys., 7, 981–1191, doi:10.5194/acp-7-981-2007, 2007.

Atkinson, R., Baulch, D. L., Cox, R. A., Crowley, J. N., Hampson, R. F., Hynes, R. G., Jenkin, M. E., Rossi, M. J., Troe, J., and Wallington, T. J.: Evaluated kinetic and photochemical data for atmospheric chemistry: Volume IV – gas phase reactions of organic halogen species, J. Phys. Chem. Ref. Data, 8, 4141–4496, 2008.

Bedjanian, Y., Le Bras, G., and Poulet, G.: Kinetic study of the $Br + IO$, $I + BrO$ and $Br + I2$ reactions. Heat of formation of the BrO radical, Chem. Phys. Lett., 266, 233–238, doi:10.1016/S0009-2614(97)01530-3, 1997.

Bell, N., Hsu, L., Jacob, D. J., Schultz, M. G., Blake, D. R., Butler, J. H., King, D. B., Lobert, J. M., and Maier-Reimer, E.: Methyl iodide: atmospheric budget and use as a tracer of marine convection in global models, J. Geophys. Res.-Atmos., 107, ACH 8–1–ACH 8–12, doi:10.1029/2001jd001151, 2002.

Bell, R. P.:The Proton in Chemistry., 2nd ed., Cornell University Press, 1973.

Bian, H. S. and Prather, M. J.: Fast-J2: accurate simulation of stratospheric photolysis in global chemical models, J. Atmos. Chem., 41, 281–296, doi:10.1023/a:1014980619462, 2002.

Bloss, W. J., Lee, J. D., Johnson, G. P., Sommariva, R., Heard, D. E., Saiz-Lopez, A., Plane, J. M. C., McFiggans, G., Coe, H., Flynn, M., Williams, P., Rickard, A. R., Fleming, L., Z.: Impact of halogen monoxide chemistry upon boundary layer OH and HO_2 concentrations at a coastal site, Geophys. Res. Lett., 32, L06814, doi:10.1029/2004GL022084, 2005.

Bloss, W. J., Rowley, D. M., Cox, R. A., and Jones, R. L.: Kinetics and products of the IO self-reaction, J. Phys. Chem. A, 105, 7840–7854, doi:10.1021/jp0044936, 2001.

Bloss, W. J., Evans, M. J., Lee, J. D., Sommariva, R., Heard, D. E., and Pilling, M. J.: The oxidative capacity of the troposphere: coupling of field measurements of OH and a global chemistry transport model, Faraday Discuss., 130, 425–436, doi:10.1039/b419090d, 2005.

Bloss, W. J., Camredon, M., Lee, J. D., Heard, D. E., Plane, J. M. C., Saiz-Lopez, A., Bauguitte, S. J.-B., Salmon, R. A., and Jones, A. E.: Coupling of HO_x, NO_x and halogen chemistry in the antarctic boundary layer, Atmos. Chem. Phys., 10, 10187–10209, doi:10.5194/acp-10-10187-2010, 2010.

Braban, C. F., Adams, J. W., Rodriguez, D., Cox, R. A., Crowley, J. N., and Schuster, G.: Heterogeneous reactions of HOI, ICl and IBr on sea salt and sea salt proxies, Phys. Chem. Chem. Phys., 9, 3136–3148, doi:10.1039/b700829e, 2007.

Breider, T. J.: Coupled Halogen-Sulfur-Aerosol Modelling in a 3D Chemical Transport Model, PhD thesis, University of Leeds, Leeds, 2010.

Butz, A., Bösch, H., Camy-Peyret, C., Chipperfield, M. P., Dorf, M., Kreycy, S., Kritten, L., Prados-Román, C., Schwärzle, J., and Pfeilsticker, K.: Constraints on inorganic gaseous iodine in the tropical upper troposphere and stratosphere inferred from balloon-borne solar occultation observations, Atmos. Chem. Phys., 9, 7229–7242, doi:10.5194/acp-9-7229-2009, 2009.

Carpenter, L. J., MacDonald, S. M., Shaw, M. D., Kumar, R., Saunders, R. W., Parthipan, R., Wilson, J., and Plane, J. M. C.: Atmospheric iodine levels influenced by sea surface emissions of inorganic iodine, Nat. Geosci., 6, 108–111, doi:10.1038/ngeo1687, 2013.

Chameides, W. L. and Davis, D. D.: Iodine: its possible role in tropospheric photochemistry, J. Geophys. Res.-Oceans, 85, 7383–7398, doi:10.1029/JC085iC12p07383, 1980.

Chance, R., Baker, A. R., Carpenter, L., and Jickells, T. D.: The distribution of iodide at the sea surface, Environ. Sci.: Processes Impacts, 16, 1841–1859, doi:10.1039/C4EM00139G, 2014.

Chuck, A. L., Turner, S. M., and Liss, P. S.: Oceanic distributions and air-sea fluxes of biogenic halocarbons in the open ocean, J. Geophys. Res.-Oceans, 110, C10022, doi:10.1029/2004jc002741, 2005.

Crowley, J. N., Ammann, M., Cox, R. A., Hynes, R. G., Jenkin, M. E., Mellouki, A., Rossi, M. J., Troe, J., and Wallington, T. J.: Evaluated kinetic and photochemical data for atmospheric chemistry: Volume V – heterogeneous reactions on solid substrates, Atmos. Chem. Phys., 10, 9059–9223, doi:10.5194/acp-10-9059-2010, 2010.

Dix, B., Baidar, S., Bresch, J., Hall, S., Schmidt, K., Wang, S.-Y., and Volkamer, R.: Detection of iodine monoxide in the tropical free troposphere, P. Natl. Acad. Sci. USA, 110, 2035–2040, doi:10.1073/pnas.1212386110, 2013.

Fiore, A. M., Naik, V., Spracklen, D. V., Steiner, A., Unger, N., Prather, M., Bergmann, D., Cameron-Smith, P. J., Cionni, I., Collins, W. J., Dalsoren, S., Eyring, V., Folberth, G. A., Ginoux, P., Horowitz, L. W., Josse, B., Lamarque, J.-F., MacKenzie, I. A., Nagashima, T., O'Connor, F. M., Righi, M., Rumbold, S. T., Shindell, D. T., Skeie, R. B., Sudo, K., Szopa, S., Takemura, T., and Zeng, G.: Global air quality and climate, Chem. Soc. Rev., 41, 6663–6683, doi:10.1039/C2CS35095E, 2012.

Fowler, D., Amann, M., Anderson, R., Ashmore, M., Cox, P., Depledge, M., Derwent, D., Grennfelt, P., Hewitt, N., Hov, O., Jenkin, M., Kelly, F., Liss, P., Pilling, M., Pyle, J., Slingo, J., and Stevenson, D.: Ground-level ozone in the 21st century: future trends, impacts and policy implications, Tech. rep., The Royal Society, 2008.

Garland, J. A. and Curtis, H.: Emission of iodine from the sea surface in the presence of ozone, J. Geophys. Res., 86, 3183–3186, doi:10.1029/JC086iC04p03183, 1981.

Gómez Martín, J. C., Spietz, P., and Burrows, J. P.: Spectroscopic studies of the I_2/O_3 photochemistry: Part 1: Determination of the absolute absorption cross sections of iodine oxides of atmospheric relevance, J. Photoch. Photobio. A, 176, 15–38, doi:10.1016/j.jphotochem.2005.09.024, 2005.

Gómez Martín, J. C., Spietz, P., and Burrows, J. P.: Kinetic and mechanistic studies of the I_2/O_3 photochemistry, J. Phys. Chem. A, 111, 306–320, doi:10.1021/jp061186c, 2007.

Gómez Martín, J. C., Mahajan, A. S., Hay, T. D., Prados-Roman, C., Ordonez, C., MacDonald, S. M., Plane, J. M. C., Sorribas, M., Gil, M., Mora, J. F. P., Reyes, M. V. A., Oram, D. E., Leedham, E., and Saiz-Lopez, A.: Iodine chemistry in the eastern Pacific marine boundary layer, J. Geophys. Res.-Atmos., 118, 887–904, doi:10.1002/jgrd.50132, 2013.

Großmann, K., Frieß, U., Peters, E., Wittrock, F., Lampel, J., Yilmaz, S., Tschritter, J., Sommariva, R., von Glasow, R., Quack, B., Krüger, K., Pfeilsticker, K., and Platt, U.: Iodine monoxide in the Western Pacific marine boundary layer, Atmos. Chem. Phys., 13, 3363–3378, doi:10.5194/acp-13-3363-2013, 2013.

Jacob, D. J.: Heterogeneous chemistry and tropospheric ozone, Atmos. Environ., 34, 2131–2159, doi:10.1016/S1352-2310(99)00462-8, 2000.

Jones, C. E., Hornsby, K. E., Sommariva, R., Dunk, R. M., Von Glasow, R., McFiggans, G., and Carpenter, L. J.: Quantifying the contribution of marine organic gases to atmospheric iodine, Geophys. Res. Lett., 37, L18804, doi:10.1029/2010gl043990, 2010.

Kaltsoyannis, N. and Plane, J. M. C.: Quantum chemical calculations on a selection of iodine-containing species (IO, OIO, INO_3, $(IO)_2$, I_2O_3, I_2O_4 and I_2O_5) of importance in the atmosphere, Phys. Chem. Chem. Phys., 10, 1723–1733, 2008.

Kim, K.-H., Shon, Z.-H., Nguyen, H. T., and Jeon, E.-C.: A review of major chlorofluorocarbons and their halocarbon alternatives in the air, Atmos. Environ., 45, 1369–1382, doi:10.1016/j.atmosenv.2010.12.029, 2011.

Law, K. S. and Sturges, W. T.: Scientific Assessment of Ozone Depletion, 2006 Chapter 2: Halogenated Very Short-Lived Substances, Tech. rep., 2006.

Lawler, M. J., Mahajan, A. S., Saiz-Lopez, A., and Saltzman, E. S.: Observations of I_2 at a remote marine site, Atmos. Chem. Phys., 14, 2669–2678, doi:10.5194/acp-14-2669-2014, 2014.

Lelieveld, J. and Dentener, F. J.: What controls tropospheric ozone?, J. Geophys. Res.-Atmos., 105, 3531–3551, doi:10.1029/1999JD901011, 2000.

Liu, H., Jacob, D. J., Bey, I., and Yantosca, R. M.: Constraints from 210Pb and 7Be on wet deposition and transport in a global three-dimensional chemical tracer model driven by assimilated meteorological fields, J. Geophys. Res.-Atmos., 106, 12109–12128, doi:10.1029/2000JD900839, 2001.

MacDonald, S. M., Gómez Martín, J. C., Chance, R., Warriner, S., Saiz-Lopez, A., Carpenter, L. J., and Plane, J. M. C.: A laboratory characterisation of inorganic iodine emissions from the sea surface: dependence on oceanic variables and parameterisation for global modelling, Atmos. Chem. Phys., 14, 5841–5852, doi:10.5194/acp-14-5841-2014, 2014.

Mahajan, A. S., Oetjen, H., Saiz-Lopez, A., Lee, J. D., McFiggans, G. B., and Plane, J. M. C.: Reactive iodine species in a semi-polluted environment, Geophys. Res. Lett., 36, L16803, doi:10.1029/2009GL038018, 2009.

Mahajan, A. S., Plane, J. M. C., Oetjen, H., Mendes, L., Saunders, R. W., Saiz-Lopez, A., Jones, C. E., Carpenter, L. J., and McFiggans, G. B.: Measurement and modelling of tropospheric reactive halogen species over the tropical Atlantic Ocean, Atmos. Chem. Phys., 10, 4611–4624, doi:10.5194/acp-10-4611-2010, 2010.

Mahajan, A. S., Gómez Martín, J. C., Hay, T. D., Royer, S.-J., Yvon-Lewis, S., Liu, Y., Hu, L., Prados-Roman, C., Ordóñez, C., Plane, J. M. C., and Saiz-Lopez, A.: Latitudinal distribution of reactive iodine in the Eastern Pacific and its link to open ocean sources, Atmos. Chem. Phys., 12, 11609–11617, doi:10.5194/acp-12-11609-2012, 2012.

Mao, J., Jacob, D. J., Evans, M. J., Olson, J. R., Ren, X., Brune, W. H., Clair, J. M. St., Crounse, J. D., Spencer, K. M., Beaver, M. R., Wennberg, P. O., Cubison, M. J., Jimenez, J. L., Fried, A., Weibring, P., Walega, J. G., Hall, S. R., Weinheimer, A. J., Cohen, R. C., Chen, G., Crawford, J. H., McNaughton, C., Clarke, A. D., Jaeglé, L., Fisher, J. A., Yantosca, R. M., Le Sager, P., and Carouge, C.: Chemistry of hydrogen oxide radicals (HO_x) in the Arctic troposphere in spring, Atmos. Chem. Phys., 10, 5823–5838, doi:10.5194/acp-10-5823-2010, 2010.

Mao, J., Paulot, F., Jacob, D. J., Cohen, R. C., Crounse, J. D., Wennberg, P. O., Keller, C. A., Hudman, R. C., Barkley, M. P., and Horowitz, L. W.: Ozone and organic nitrates over the eastern United States: sensitivity to isoprene chemistry, J. Geophys. Res.-Atmos., 118, 11256–11268, doi:10.1002/jgrd.50817, 2013.

McFiggans, G., Plane, J. M. C., Allan, B. J., Carpenter, L. J., Coe, H., and O'Dowd, C.: A modeling study of iodine chemistry in the marine boundary layer, J. Geophys. Res.-Atmos., 105, 14371–14385, doi:10.1029/1999JD901187, 2000.

McFiggans, G., Bale, C. S. E., Ball, S. M., Beames, J. M., Bloss, W. J., Carpenter, L. J., Dorsey, J., Dunk, R., Flynn, M. J., Furneaux, K. L., Gallagher, M. W., Heard, D. E., Hollingsworth, A. M., Hornsby, K., Ingham, T., Jones, C. E., Jones, R. L., Kramer, L. J., Langridge, J. M., Leblanc, C., LeCrane, J.-P., Lee, J. D., Leigh, R. J., Longley, I., Mahajan, A. S., Monks, P. S., Oetjen, H., Orr-Ewing, A. J., Plane, J. M. C., Potin, P., Shillings, A. J. L., Thomas, F., von Glasow, R., Wada, R., Whalley, L. K., and Whitehead, J. D.: Iodine-mediated coastal particle formation: an overview of the Reactive Halogens in the Marine Boundary Layer (RHaMBLe) Roscoff coastal study, Atmos. Chem. Phys., 10, 2975–2999, doi:10.5194/acp-10-2975-2010, 2010.

McLinden, C. A., Olsen, S. C., Hannegan, B., Wild, O., Prather, M. J., and Sundet, J.: Stratospheric ozone in 3-D models: a simple chemistry and the cross-tropopause flux, J. Geophys. Res., 105, 14653, doi:10.1029/2000JD900124, 2000.

Murray, B. J., Haddrell, A. E., Peppe, S., Davies, J. F., Reid, J. P., O'Sullivan, D., Price, H. C., Kumar, R., Saunders, R. W., Plane, J. M. C., Umo, N. S., and Wilson, T. W.: Glass formation and unusual hygroscopic growth of iodic acid solution droplets with relevance for iodine mediated particle formation in the marine boundary layer, Atmos. Chem. Phys., 12, 8575–8587, doi:10.5194/acp-12-8575-2012, 2012.

Ordóñez, C., Lamarque, J.-F., Tilmes, S., Kinnison, D. E., Atlas, E. L., Blake, D. R., Sousa Santos, G., Brasseur, G., and Saiz-Lopez, A.: Bromine and iodine chemistry in a global chemistry-climate model: description and evaluation of very short-lived oceanic sources, Atmos. Chem. Phys., 12, 1423–1447, doi:10.5194/acp-12-1423-2012, 2012.

Parrella, J. P., Jacob, D. J., Liang, Q., Zhang, Y., Mickley, L. J., Miller, B., Evans, M. J., Yang, X., Pyle, J. A., Theys, N., and Van Roozendael, M.: Tropospheric bromine chemistry: implications for present and pre-industrial ozone and mercury, Atmos. Chem. Phys., 12, 6723–6740, doi:10.5194/acp-12-6723-2012, 2012.

Prados-Roman, C., Cuevas, C. A., Fernandez, R. P., Kinnison, D. E., Lamarque, J-F., and Saiz-Lopez, A.: A negative feedback between anthropogenic ozone pollution and enhanced ocean emissions of iodine, Atmos. Chem. Phys., 15, 2215–2224, doi:10.5194/acp-15-2215-2015, 2015a.

Prados-Roman, C., Cuevas, C. A., Hay, T., Fernandez, R. P., Mahajan, A. S., Royer, S.-J., Galí, M., Simó, R., Dachs, J., Großmann, K., Kinnison, D. E., Lamarque, J.-F., and Saiz-Lopez, A.: Iodine oxide in the global marine boundary layer, Atmos. Chem. Phys., 15, 583–593, doi:10.5194/acp-15-583-2015, 2015b.

Puentedura, O., Gil, M., Saiz-Lopez, A., Hay, T., Navarro-Comas, M., Gómez-Pelaez, A., Cuevas, E., Iglesias, J., and Gomez, L.: Iodine monoxide in the north subtropical free troposphere, Atmos. Chem. Phys., 12, 4909–4921, doi:10.5194/acp-12-4909-2012, 2012.

Read, K. A., Mahajan, A. S., Carpenter, L. J., Evans, M. J., Faria, B. V. E., Heard, D. E., Hopkins, J. R., Lee, J. D., Moller, S. J., Lewis, A. C., Mendes, L., McQuaid, J. B., Oetjen, H., Saiz-Lopez, A., Pilling, M. J., and Plane, J. M. C.: Extensive halogen-mediated ozone destruction over the tropical Atlantic Ocean, Nature, 453, 1232–1235, doi:10.1038/nature07035, 2008.

Riffault, V., Bedjanian, Y., and Poulet, G.: Kinetic and mechanistic study of the reactions of OH with IBr and HOI, J. Photoch. Photobio. A, 176, 155–161, doi:10.1016/j.jphotochem.2005.09.002, 2005.

Saiz-Lopez, A., Plane, J. M. C., McFiggans, G., Williams, P. I., Ball, S. M., Bitter, M., Jones, R. L., Hongwei, C., and Hoffmann, T.: Modelling molecular iodine emissions in a coastal marine environment: the link to new particle formation, Atmos. Chem. Phys., 6, 883–895, doi:10.5194/acp-6-883-2006, 2006.

Saiz-Lopez, A., Chance, K., Liu, X., Kurosu, T. P., and Sander, S. P.: First observations of iodine oxide from space, Geophys. Res. Lett., 34, L12812, doi:10.1029/2007gl030111, 2007.

Saiz-Lopez, A., Plane, J. M. C., Mahajan, A. S., Anderson, P. S., Bauguitte, S. J.-B., Jones, A. E., Roscoe, H. K., Salmon, R. A., Bloss, W. J., Lee, J. D., and Heard, D. E.: On the vertical distribution of boundary layer halogens over coastal Antarctica: implications for O_3, HO_x, NO_x and the Hg lifetime, Atmos. Chem. Phys., 8, 887–900, doi:10.5194/acp-8-887-2008, 2008.

Saiz-Lopez, A., Lamarque, J.-F., Kinnison, D. E., Tilmes, S., Ordóñez, C., Orlando, J. J., Conley, A. J., Plane, J. M. C., Mahajan, A. S., Sousa Santos, G., Atlas, E. L., Blake, D. R., Sander, S. P., Schauffler, S., Thompson, A. M., and Brasseur, G.: Estimating the climate significance of halogen-driven ozone loss in the tropical marine troposphere, Atmos. Chem. Phys., 12, 3939–3949, doi:10.5194/acp-12-3939-2012, 2012a.

Saiz-Lopez, A., Plane, J. M. C., Baker, A. R., Carpenter, L. J., von Glasow, R., Martin, J. C. G., McFiggans, G., and Saunders, R. W.: Atmospheric chemistry of iodine, Chem. Rev., 112, 1773–1804, doi:10.1021/cr200029u, 2012b.

Saiz-Lopez, A., Fernandez, R. P., Ordóñez, C., Kinnison, D. E., Gómez Martín, J. C., Lamarque, J.-F., and Tilmes, S.: Iodine chemistry in the troposphere and its effect on ozone, Atmos. Chem. Phys. Discuss., 14, 19985–20044, doi:10.5194/acpd-14-19985-2014, 2014.

Sander, R.: Compilation of Henry's Law Constants for Inorganic and Organic Species of Potential Importance in Environmental Chemistry, ~~available at:(last access: 1 January 2013), 1999.~~ Atmos. Chem. Phys., 15, 4399-4981, doi:10.5194/acp-15-4399-2015, 2015.

Sander, R., Vogt, R., Harrris, G. W., and Crutzen, P. J.: Modelling the chemistry of ozone, halogen compounds, and hydrocarbons in the arctic troposphere during spring, Tellus B, 49, 522–532, doi:10.1034/j.1600-0889.49.issue5.8.x, 1997.

Sander, S. P., Golden, D. M., Kurylo, M. J., Moortgat, G. K., Wine, P. H., Ravishankara, A. R., Kolb, C. E., Molina, M. J., Finlayson-Pitts, B. J., Huie, R. E., and Orkin, V. L.: Chemical kinetics and photochemical data for use, in: Atmospheric Studies Evaluation, Number 15, 2006.

Sander, S. P., Friedl, R. R., Abbatt, J. P. D., Barker, J. R., Burkholder, J. B., Golden, D. M., Kolb, C. E., Kurylo, M. J., Moortgat, G. K., Wine, P. H., Huie, R. E., and Orkin, V. L.: Chemical kinetics and photochemical data for use in atmospheric studies, Evaluation Number 17, Tech. rep., NASA Jet Propulsion Laboratory, 2011.

Schönhardt, A., Richter, A., Wittrock, F., Kirk, H., Oetjen, H., Roscoe, H. K., and Burrows, J. P.: Observations of iodine monoxide columns from satellite, Atmos. Chem. Phys., 8, 637–653, doi:10.5194/acp-8-637-2008, 2008.

Shaw, M. D. and Carpenter, L. J.: Modification of ozone deposition and I_2 emissions at the air–aqueous interface by dissolved organic carbon of marine origin, Environ. Sci. Technol., 47, 10947–10954, doi:10.1021/es4011459, 2013.

Sofen, E. D. and Evans, M. J.: Surface O_3 dataset, Earth Syst. Sci. Data Discuss., in preparation, 2015.

Sommariva, R., Bloss, W. J., and von Glasow, R.: Uncertainties in gas-phase atmospheric iodine chemistry, Atmos. Environ., 57, 219–232, doi:10.1016/j.atmosenv.2012.04.032, 2012.

Spietz, P., Gómez Martín, J. C., and Burrows, J. P.: Spectroscopic studies of the I_2/O_3 photochemistry: Part 2. Improved spectra of iodine oxides and analysis of the IO absorption spectrum, J. Photoch. Photobio. A, 176, 50–67, doi:10.1016/j.jphotochem.2005.08.023, 2005.

Stuart, A. L. and Jacobson, M. Z.: A timescale investigation of volatile chemical retention during hydrometeor freezing: nonrime freezing and dry growth riming without spreading, J. Geophys. Res., 108, 4178, doi:10.1029/2001JD001408, 2003.

Vogt, R., Sander, R., Von Glasow, R., and Crutzen, P. J.: Iodine chemistry and its role in halogen activation and ozone loss in the marine boundary layer: a model study, J. Atmos. Chem., 32, 375–395, doi:10.1023/a:1006179901037, 1999.

Volkamer, R., Baidar, S., Campos, T. L., Coburn, S., DiGangi, J. P., Dix, B., Eloranta, E. W., Koenig, T. K., Morley, B., Ortega, I., Pierce, B. R., Reeves, M., Sinreich, R., Wang, S., Zondlo, M. A., and Romashkin, P. A.: Aircraft measurements of BrO, IO, glyoxal, NO_2, H_2O, O_2-O_2 and aerosol extinction profiles in the tropics: comparison with aircraft-/ship-based in situ and lidar measurements, Atmos. Meas. Tech., 8, 2121–2148, doi:10.5194/amt-8-2121-2015, 2015.

von Glasow, R., Sander, R., Bott, A., and Crutzen, P. J.: Modeling halogen chemistry in the marine boundary layer 2. Interactions with sulfur and the cloud-covered MBL, J. Geophys. Res.-Atmos., 107, 4323, doi:10.1029/2001JD000943, 2002.

von Glasow, R., von Kuhlmann, R., Lawrence, M. G., Platt, U., and Crutzen, P. J.: Impact of reactive bromine chemistry in the troposphere, Atmos. Chem. Phys., 4, 2481–2497, doi:10.5194/acp-4-2481-2004, 2004.

Voulgarakis, A., Naik, V., Lamarque, J.-F., Shindell, D. T., Young, P. J., Prather, M. J., Wild, O., Field, R. D., Bergmann, D., Cameron-Smith, P., Cionni, I., Collins, W. J., Dalsøren, S. B., Doherty, R. M., Eyring, V., Faluvegi, G., Folberth, G. A., Horowitz, L. W., Josse, B., MacKenzie, I. A., Nagashima, T., Plummer, D. A., Righi, M., Rumbold, S. T., Stevenson, D. S., Strode, S. A., Sudo, K., Szopa, S., and Zeng, G.: Analysis of present day and future OH and methane lifetime in the ACCMIP simulations, Atmos. Chem. Phys., 13, 2563–2587, doi:10.5194/acp-13-2563-2013, 2013.

Wang, S.-Y., Schmidt, J., Baidar, S., Coburn, S., Dix, B., Koenig, T., Apel, E., Bowdalo, D., Campos, T., Eloranta, E., Evans, M., DiGangii, J., Zondlo, M., Gao, R.-S., Haggerty, J., Hall, S., Hornbrook, R., Jacob, D., Morley, B., Pierce, B., Reeves, M., Romashkin, P., ter Schure, A., and Volkamer, R.: Active and widespread halogen chemistry in the tropical and subtropical free troposphere, P. Natl. Acad. Sci. USA, 112, 9281–9286, doi:10.1073/pnas.1505142112, 2015.

Wesely, M. L.: Parameterization of surface resistances to gaseous dry deposition in regional-scale numerical models, Atmos. Environ., 23, 1293–1304, doi:10.1016/0004-6981(89)90153-4, 1989.

WOUDC: WOUDC Ozone Monitoring Community, World Meteorological Organization-Global Atmosphere Watch Program (WMO-GAW)/World Ozone and Ultraviolet Radiation Data Centre (WOUDC) [Data], doi:10.14287/10000001, available at: http://www.woudc.org, last access: 1 October 2014.

Young, P. J., Archibald, A. T., Bowman, K. W., Lamarque, J.-F., Naik, V., Stevenson, D. S., Tilmes, S., Voulgarakis, A., Wild, O., Bergmann, D., Cameron-Smith, P., Cionni, I., Collins, W. J., Dalsøren, S. B., Doherty, R. M., Eyring, V., Faluvegi, G., Horowitz, L. W., Josse, B., Lee, Y. H., MacKenzie, I. A., Nagashima, T., Plummer, D. A., Righi, M., Rumbold, S. T., Skeie, R. B., Shindell, D. T., Strode, S. A., Sudo, K., Szopa, S., and Zeng, G.: Pre-industrial to end 21st century projections of tropospheric ozone from the Atmospheric Chemistry and Climate Model Intercomparison Project (ACCMIP), Atmos. Chem. Phys., 13, 2063–2090, doi:10.5194/acp-13-2063-2013, 2013.

Ziska, F., Quack, B.,Abrahamsson, K, Archer, S. D.,Atlas, E.,Bell, T.,Butler, J. H.,Carpenter, L. J., Jones, C. E.,Harris, N. R. P.,Hepach, H.,Heumann, K. G.,Hughes, C.,Kuss, J.,Krüger, K., Liss, P.,Moore, R. M.,Orlikowska, A.,Raimund, S.,Reeves, C. E.,Reifenhäuser, W.,Robinson, A D.,Schall, Global sea-to-air flux climatology for bromoform, dibromomethane and methyl iodide, Atmos. Chem. Phys., 17, 8915–8934, doi:10.5194/acp-13-8915-2013, 2013.

Table 1. Total simulated emissions for iodinated species.~~Values are given as annual totals in Tg of iodine.~~

Species	Emissions Tg I yr^{-1}
CH_3I	0.26
CH_2I_2	0.11
CH_2ICl	0.18
CH_2IBr	0.05
I_2	0.32
HOI	2.91
Total	3.83

Table 2. Henry's law coefficients and molar heats of formation of iodine species. Where Henry's law constant equals infinity a very large values is used within the model (1×10^{20} M atm^{-1}). The INO_2 Henry's law constant is assumed equal to that of $BrNO_3$, from Sander (2015), by analogy. For I_2O_X (~~$X = 2, 3, 4$~~ $X = 2, 3, 4$) a Henry's law constant of infinity is assumed by analogy with INO_3. (∗) Effective henry's law of HI is calculated for acid conditions through $K^*_H(T) = K_H(T) \times (1 + \frac{K_a}{[H^+]})$, where K_a =1×10^9 M is the acid dissociation constant (Bell, 1973).

Num.	Species	Henry's Law Constant M atm^{-1}	Reference	Molar Heat of Formation 298 K/R (K)	Reference
D1	HOI	1.53×10^4	Sander (2015)	-8.37×10^3	Sander et al. (2006)
D2	HI	~~2.50×10^1~~ 2.35×10^0(*)	Sander (2015)	-3.19×10^3	Sander et al. (2006)
D3	INO_3	∞	Vogt et al. (1999)	-3.98×10^4	Kaltsoyannis and Plane (2008)
D4	I_2O_2	∞	see caption text	-1.89×10^4	Kaltsoyannis and Plane (2008)
D5	I_2	2.63×10^0	Sander (2015)	-7.51×10^3	Sander et al. (2006)
D6	INO_2	3.00×10^{-1}	see caption text	-7.24×10^3	Sander et al. (2006)
D7	I_2O_3	∞	see caption text	-7.70×10^3	Kaltsoyannis and Plane (2008)
D8	I_2O_4	∞	see caption text	-1.34×10^4	Kaltsoyannis and Plane (2008)

Table 3. Bimolecular and unimolecular iodine reactions. These are given in the Arrhenius form with the rate equal to $A \cdot \exp(\frac{Ea}{RT})$. Unknown values are represented by a dash and these set to zero in the model, reducing the exponent to 1. The bi-molecular reactions with an M in them represent termolecular reactions where the pressure dependence is not known or are uni-molecular decomposition reactions. Reactions included, but not in IUPAC/JPL are discussed further in Section A1.1.

Rxn ID
M1
M2
M3
M4
M5
M6
M7
M8
M9
M10
M11
M12
M13
M14
M15
M16
M17
M18
~~Termolecular iodine reactions.The lower pressure limit rate (k_0) is given by: $A_0 \cdot \exp(\frac{Ea_0}{RT}) \cdot (\frac{300}{T})^x$. The high pressure limit rate k($_\infty$)~~
~~T2~~ M20
~~T3*~~ M21
~~T4~~ M22
~~T5*~~ M23
~~T6~~ M24
~~T7~~ M25
~~T8~~ M26

Table 4. Termolecular iodine reactions. The lower pressure limit rate (k_0) is given by: $A_0 \cdot \exp(\frac{Ea}{RT}) \cdot (\frac{300}{T})^x$. The high pressure limit is given by k_∞. Fc characterises the fall off curve of the reaction as described by Atkinson et al. (2007). Unknown values are represented by a dash and these set to zero in the model, reducing the exponent to 1.

Rxn ID	~~–~~Reaction ~~–~~	~~–~~A_0 ~~–~~cm^6 molecules^{-2} s^{-1}	~~0.60~~ Ea/R ~~–~~K	~~T9~~ x ~~–~~	k_∞ cm^3 molecules^{-1} s^{-1}	~~1.50×10^{-10}~~ Fc	~~–~~Citation
~~T10~~ T1	$I + NO + M \rightarrow INO + M$	~~1.00×10^{12}~~ 1.80×10^{-32}	~~–9770~~ 300	~~–~~1	~~–~~1.70×10^{-11}	~~–~~0.60	Atkinson et al. (2007)
~~T11~~ T2	$I + NO_2 + M \rightarrow INO_2 + M$	~~2.50×10^{14}~~ 3.00×10^{-31}	~~–9770~~ 300	~~–~~1	~~–~~6.60×10^{-11}	~~–~~0.63	~~0.60~~ Atkinson et al. (2007)
~~T12~~ T3	$IO + NO_2 + M \rightarrow INO_3 + M$	~~3.80×10^{-2}~~ 7.70×10^{-31}	–	~~–~~5	~~–~~1.60×10^{-11}	~~–~~0.40	~~–~~Atkinson et al. (2007)

Table 5. Photolysis reactions of iodine species. For I_2O_X (~~$X = 2,3,4$~~$x = 2,3,4$) the cross-section of INO_3 is used as described in Sect. 2.4.

ID	Reaction	Reference cross-section
J1	$I_2 + h\nu \rightarrow 2I$	Sander et al. (2011)
J2	$HOI + h\nu \rightarrow I + OH$	Sander et al. (2011)
J3	$IO + h\nu \rightarrow I + [O_3]$	Sander et al. (2011)
J4	$OIO + h\nu \rightarrow I + O_2$	Sander et al. (2011)
J5	$INO + h\nu \rightarrow I + NO$	Sander et al. (2011)
J6	$INO_2 + h\nu \rightarrow I + NO_2$	Sander et al. (2011)
J7	$INO_3 + h\nu \rightarrow I + NO_3$	Sander et al. (2011)
J8	$I_2O_2 + h\nu \rightarrow I + OIO$	see ~~Sect. 2.4~~ caption
J9	$CH_3I + h\nu \rightarrow I + CH_2O_2$	Sander et al. (2011)
J10	$CH_2I_2 + h\nu \rightarrow 2I + (CH_2)$	Sander et al. (2011)
J11	$CH_2ICl + h\nu \rightarrow I + (CH_2Cl)$	Sander et al. (2011)
J12	$CH_2IBr + h\nu \rightarrow I + (CH_2Br)$	Sander et al. (2011)
J20	$I_2O_4 + h\nu \rightarrow 2OIO$	see ~~Sect. 2.4~~ caption
J21	$I_2O_3 + h\nu \rightarrow OIO + IO$	see ~~Sect. 2.4.~~ caption

Table 6. Heterogeneous reactions of iodine species. Where measured values have not been reported estimated values are used and no reference is given, further detail on uptake choices is in Sect. A1.2. Stared (*) reactions proceed only on sea-salt aerosols.

ID	Reaction	Reactive uptake coefficient (γ)	Reference
K1	HI → iodine aerosol	0.10^*	Crowley et al. (2010)
K2	$INO_3 \rightarrow 0.5I_2$	0.01^*	see caption text
K3	$HOI \rightarrow 0.5I_2$	0.01^*	Sander et al. (2011)
K4	$INO_2 \rightarrow 0.5I_2$	0.02^*	see caption text
K5	I_2O_2 → iodine aerosol	0.02	see caption text
K6	I_2O_4 → iodine aerosol	0.02	see caption text
K7	I_2O_3 → iodine aerosol	0.02	see caption text

Table 7. Comparison between global tropospheric O_X budgets of ~~standard GEOS-Chem (v9-2)~~simulations “BROMINE”, “Br+I” , “IODINE” and “NOHAL” are described here. ~~which~~ “BROMINE” includes just bromine chemistry~~and the iodine simulation described here~~, “Br+I” which includes both iodine and bromine chemistry, “IODINE” only includes iodine chemistry, and “NOHAL” is simulation without iodine or bromine chemistry. Recent average model values from Young et al. (2013) are also shown. For the IO + BrO halogen crossover reaction we allocate half the O_3 loss to bromine and half to iodine. Values are rounded to the nearest integer value.

Scenario	~~GEOS-Chem~~ “NOHAL”	~~Iodine~~ “IODINE”	~~ACCENT~~ “BROMINE”	~~simulation (v9-2)~~ “Br+I”	~~simulation~~ ACCENT Young et al. (
O_3 burden (Tg)	390	357	367	334	340
O_X chemical Sources (Tg Yr^{-1})					
$NO + HO_2$	3667	3680	3512	3529	
$NO + CH_3O_2$	1332	1383	1269	1307	
Other O_X sources	502	518	505	521	
Total chemical O_X sources (PO_X)	5501	5581	5286	5357	5110
O_X chemical sinks (Tg Yr^{-1})					
$O_3 + h\nu + H_2O \rightarrow 2OH + O_2$	2579	2271	2425	2119	
$O_3 + HO_2 \rightarrow OH + O_2$	1391	1186	1274	1080	
$O_3 + OH \rightarrow HO_2 + O_2$	687	627	621	560	
$HOBr + h\nu \rightarrow Br + OH$	–	–	166	143	
$HOBr + HBr \rightarrow Br_2 + H_2O$ (aq. aerosol)	–	–	8	8	
$BrO + BrO \rightarrow 2Br + O_2$	–	–	12	10	
$BrO + BrO \rightarrow Br_2 + O_2$	–	–	3	3	
$BrO + OH \rightarrow Br + HO_2$	–	–	6	5	
$IO + BrO \rightarrow Br + I + O_2$	–	–	–	7	
Other bromine O_X sinks	–	–	1	1	
Total bromine O_X sinks	–	–	195	178	
$HOI + h\nu \rightarrow I + OH$	–	639	–	583	
$HOI \rightarrow 0.5I_2$ (seasalt aerosol)	–	2	–	2	
$IO + BrO \rightarrow Br + I + O_2$	–	–	–	7	
$OIO + h\nu \rightarrow I + O_2$	–	114	–	156	
Other iodine O_X sinks	–	1	–	1	
Total iodine O_X sinks	–	756	–	748	
Other O_X sinks	176	181	172	~~173~~ 179	
Total chem. O_X sinks (LO_X)	4833	5021	4687	4864	4668
O_3 $P(O_X)$-$L(O_X)$ (Tg Yr^{-1})	668	560	599	493	~~442 (aprox.)~~ 618
O_3 Dry deposition (Tg Yr^{-1})	949	850	886	791	1003
O_3 Lifetime (days)	25	22	24	22	2
O_3 STE (PO_X-LO_X-Dry dep.) (Tg Yr^{-1})	281	290	287	298	552

Table A1. Effects of sensitivity runs on relevant variables. Values are shown as percentage change from the ~~iodine~~ simulation with both iodine and bromine chemistry ("Br+I") in the troposphere as global means unless otherwise stated. MBL = Marine Boundary Layer (900 ~~< hPa~~hPa $<$ p), O_X is defined as in ~~the text~~Footnote 1. CH_4 lifetime is calculated globally in the troposphere with respect to loss by reaction with OH.

	Mean IO MBL surface concentration	Chem. O_X loss (LO_X)	Chem. O_X prod. (PO_X)	PO_X -LO_X	O_3 burden	O_3 deposition
NOHAL	-100.00	2.34	-0.75	40.91	15.99	17.75
BROMINE	-100.00	-1.79	-3.90	24.50	9.12	10.42
IODINE	9.63	3.87	2.89	16.16	6.90	6.87
Br-I	0.00	0.00	0.00	0.00	0.00	0.00
Just org. I	−83.45	−1.64	−3.11	17.69	5.53	7.19
I_2O_X loss (γ) ×2	−4.26	−0.15	−0.28	1.61	0.54	0.59
I_2O_X loss (γ)/2	3.93	0.13	0.24	−1.34	−0.44	−0.52
Het. cycle (γ) ×2	2.21	0.04	0.16	−1.61	−0.69	−0.56
Het. cycle (γ)/2	−1.84	−0.06	−0.14	1.07	0.56	0.45
No Het. cycle	−48.03	−1.15	−2.20	12.60	4.09	5.23
Sulphate Uptake	−22.49	−1.25	−2.26	12.06	4.54	4.94
Ocean iodide	−34.28	−0.66	−1.26	7.24	2.06	3.01
I_2O_X X-sections ×2	4.30	0.11	0.22	−1.34	−0.40	−0.47
I_2O_X exp. X-sections	6.73	0.19	0.35	−1.88	−0.60	−0.73
No I_2O_X Photolysis	−39.35	−1.10	−2.12	12.33	5.05	4.86
MBL BrO 2 pmol/mol	−6.78	−3.59	−2.71	−15.28	−3.73	−6.03

Table A1. Continued.

	OH mean concentration	HO_2 mean concentration	HO_2 /OH	I_Y lifetime	IO_X lifetime	I_Y burden	CH_4 lifetime
NOHAL	2.49	8.44	5.81	-100.00	105.16	-100.00	-3.73
BROMINE	-1.65	5.72	7.50	-100.00	89.64	-100.00	0.80
IODINE	4.30	2.31	-1.91	-1.31	-1.82	6.96	-4.67
Br-I	0.00	0.00	0.00	0.00	0.00	0.00	0.00
Just org. I	−0.64	3.53	4.19	123.92	16.09	−64.26	0.21
I_2O_X loss (γ) ×2	−0.08	0.27	0.36	−8.38	−0.93	−5.08	0.03
I_2O_X loss (γ)/2	0.05	−0.22	−0.27	8.00	0.55	4.27	−0.01
Het. cycle (γ) ×2	0.09	−0.39	−0.49	4.61	1.13	5.98	0.00
Het. cycle (γ)/2	−0.09	0.32	0.41	−3.89	−0.96	−5.04	0.02
No Het. cycle	−0.47	2.58	3.07	−61.18	5.38	−46.69	0.15
Sulphate Uptake	−0.87	2.70	3.60	−59.60	0.49	−48.49	0.52
Ocean iodide	−0.17	1.22	1.39	16.90	2.77	−23.42	0.01
I_2O_X X-sections ×2	0.05	−0.20	−0.25	5.26	0.61	3.10	−0.01
I_2O_X exp. X-sections	0.08	−0.31	−0.39	8.31	0.84	4.81	−0.01
No I_2O_X Photolysis	−0.90	2.54	3.48	−46.41	−17.68	−34.58	0.32
MBL BrO 2 pmol/mol	−3.31	−1.44	1.93	−3.72	3.33	−10.07	4.17

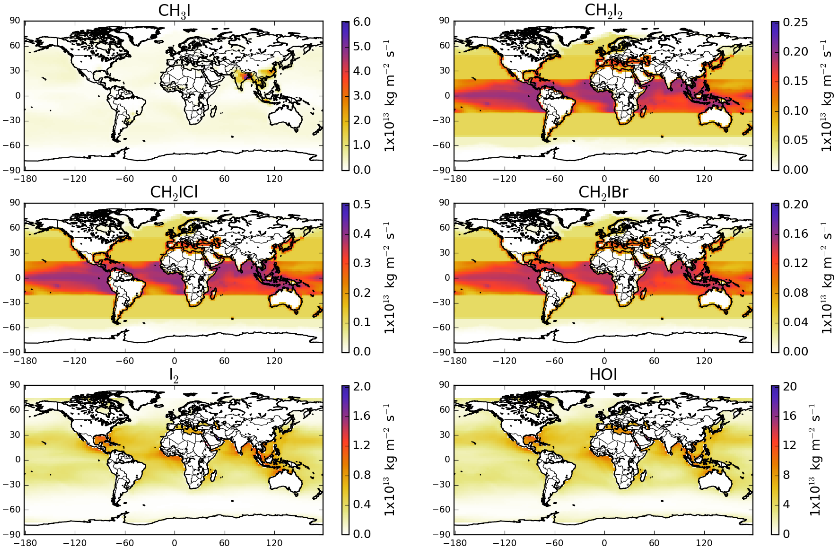

Figure 1. Annual mean ~~zonal tropospheric mixing ratios~~ surface fluxes for ~~precursor and reactive~~ iodine ~~compounds (pptv).No calculations of concentrations are made within~~ precursors in the ~~stratosphere and so that region is left blank.~~ "Br+I" simulation in kg m^{-2} s^{-1}

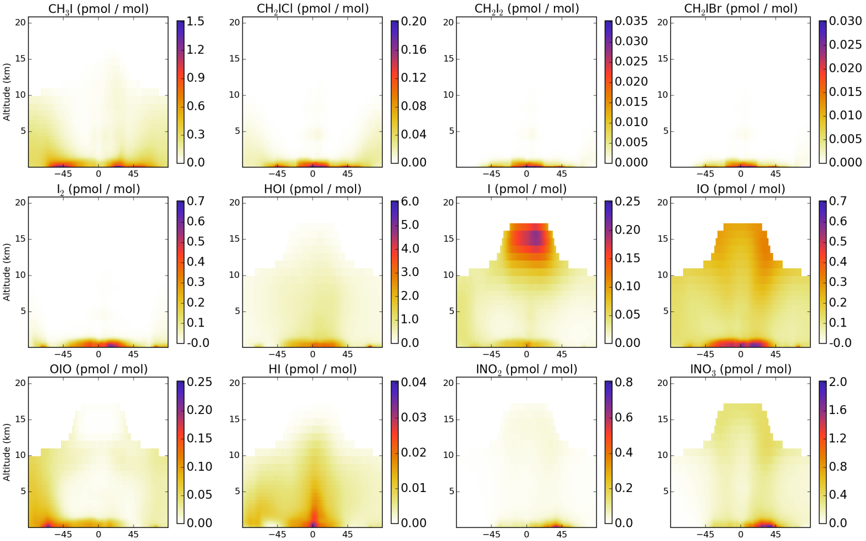

Figure 2. Annual mean zonal tropospheric mixing ratios for precursor and reactive iodine compounds (pmol/mol) in the simulation with both iodine and bromine chemistry (“Br+I”). No calculations of concentrations are made within the stratosphere and so that region is left blank.

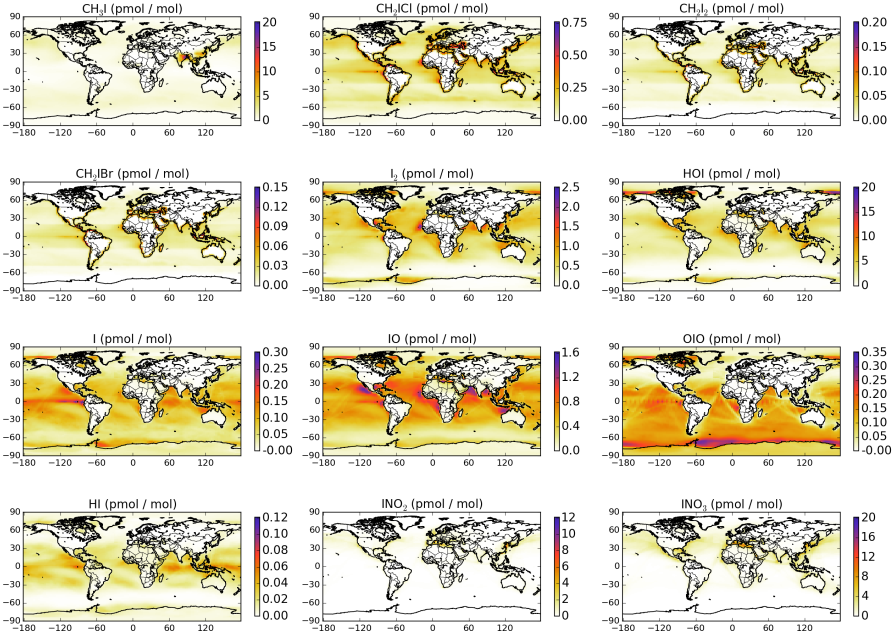

Figure 3. Annual mean surface mixing ratios for precursor and reactive iodine (~~pptv~~pmol/mol) in the simulation with both iodine and bromine chemistry ("Br+I").

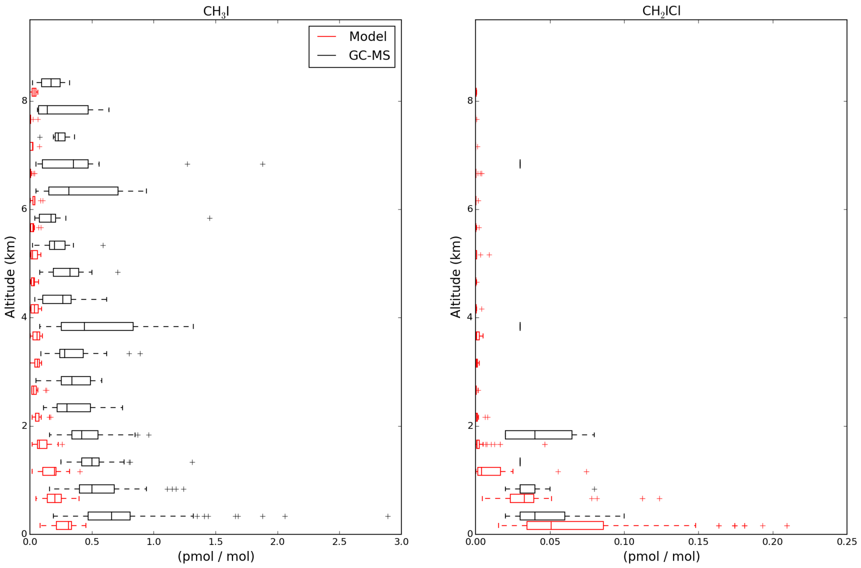

Figure 4. Vertical comparison of observations from the CAST (Combined Airborne Studies in the Tropics) campaign in the mid Pacific (Guam). The observations are shown in black and ~~modelled~~ simulated values with both iodine and bromine chemistry (“Br+I”) in red. Values are considered in 0.5 km bins, with observations and modelled values at the same location and time (as described in section 2) shown side-by-side around the mid point of each bin. The observations are from the FAAM BAE-146 research aircraft ~~Whole Air Samples (WAS)~~ whole air samples analysed by Gas Chromatography-Mass Spectrometry (GC-MS). The boxplot extents give the inter-quartile range, with the median shown within the box. The whiskers give the most extreme point within 1.5 times the inter-quartile range.

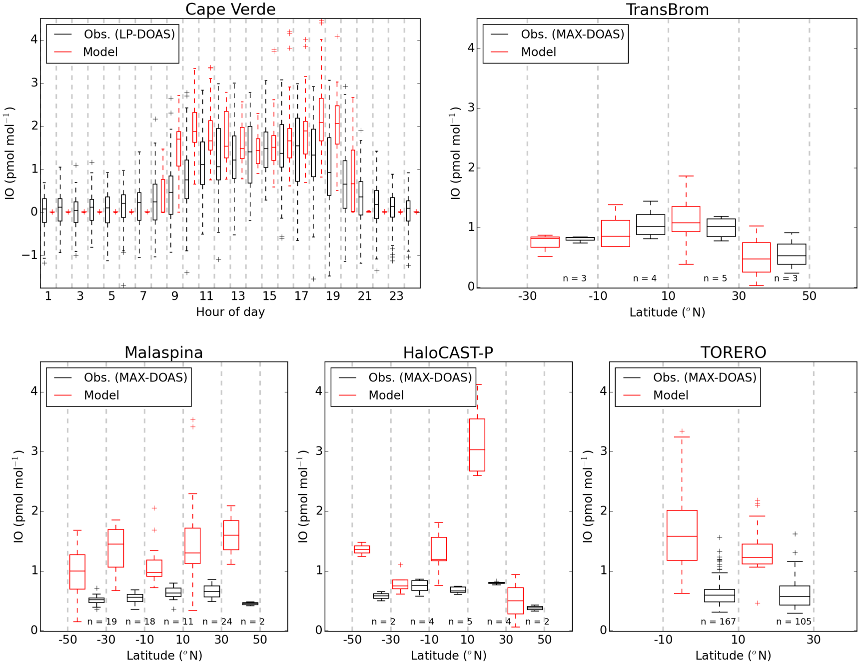
Cape Verde
Obs. (LP-DOAS)
Model
IO (pmol mol^{-1})
Hour of day
1
3
5
7
9
11
13
15
17
19
21
23
−1
0
1
2
3
4
TransBrom
Obs. (MAX-DOAS)
Model
IO (pmol mol^{-1})
Latitude (^{o}N)
-30
-10
10
30
50
n = 3
n = 4
n = 5
n = 3
Malaspina
Obs. (MAX-DOAS)
Model
n = 19
n = 18
n = 11
n = 24
n = 2
-50
-30
-10
10
30
50
Latitude (^{o}N)
HaloCAST-P
Obs. (MAX-DOAS)
Model
n = 2
n = 4
n = 5
n = 4
n = 2
-50
-30
-10
10
30
50
Latitude (^{o}N)
TORERO
Obs. (MAX-DOAS)
Model
n = 167
n = 105
-10
10
30
Latitude (^{o}N)

Figure 5. Iodine oxide (IO) surface observations (red) by campaign compared against ~~model~~ the simulation with both iodine and bromine chemistry ("Br+I", black). Cape Verde measurements are shown against hour of day and others are shown as a function of latitude. Values are considered in 20° bins, with observations and modelled values at the same location and time (as described in section 2) shown side-by-side around the mid point of each bin. Extents of bins are highlighted with grey dashed lines. Observations are from Cape Verde (Tropical Atlantic Mahajan et al., 2010; Read et al., 2008), Transbrom (West Pacific, Großmann et al., 2013), the Malaspina circumnavigation (Prados-Roman et al., 2015b), ~~and~~ HaloCAST-P (East Pacific, Mahajan et al., 2012), and TORERO ship (East Pacific, (Volkamer et al., 2015)). Number of data points within latitudinal bin are shown as "n". The boxplot extents give the inter-quartile range, with the median shown within the box. The whiskers give the most extreme point within 1.5 times the inter-quartile range.

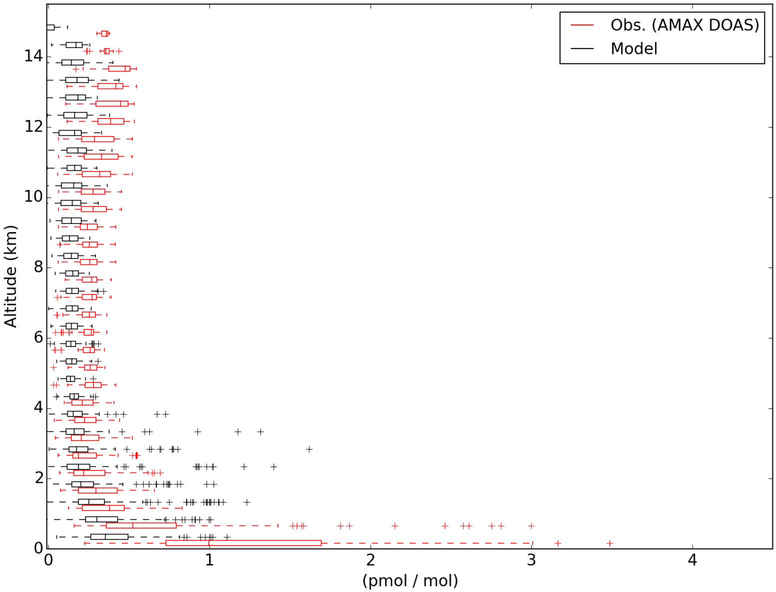

Figure 6. Vertical comparison of ~~modelled~~ the simulation with both iodine and bromine chemistry ("Br+I") and measured iodine oxide (IO) during ~~the~~ TORERO ~~research~~ aircraft campaign ~~.~~(Volkamer et al., 2015; Wang et al., 2015). Model and observations are in red and black respectively. Values are considered in 0.5 km bins, with observations and modelled values at the same location and time (as described in section 2) shown side-by-side around the mid point of each bin. Measurements were taken aboard the NSF/NCAR GV research aircraft by the University of Colorado airborne Multi-Axis DOAS instrument (CU AMAX-DOAS) ~~as part of the TORERO campaign~~ in the eastern Pacific in January and February ~~2012.~~ 2012 (Volkamer et al., 2015; Wang et al., 2015) . The boxplot extents give the inter-quartile range, with the median shown within the box. The whiskers give the most extreme point within 1.5 times the inter-quartile range.

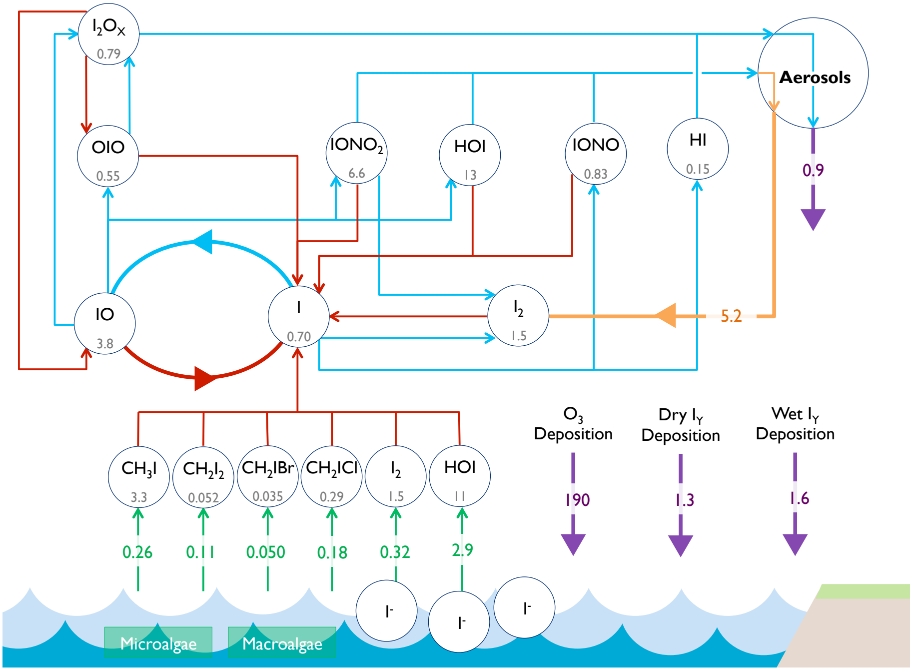

Figure 7. Schematic representation of implemented iodine chemistry in the simulation with both iodine and bromine chemistry ("Br+I"). Average global annual mean burdens (Gg I) are shown below key I_Y species, with fluxes (Tg I yr^{-1}) shown on arrows. Red lines = photolysis, blue = chemical pathways, green lines = emission source, orange lines = heterogeneous pathway, and purple lines = depositional pathway. This equates to a total iodine source and sink of $3.8\,\text{Tg I yr}^{-1}$. O_3 deposition in Tg is also shown to illustrate the driving force behind the inorganic emissions.

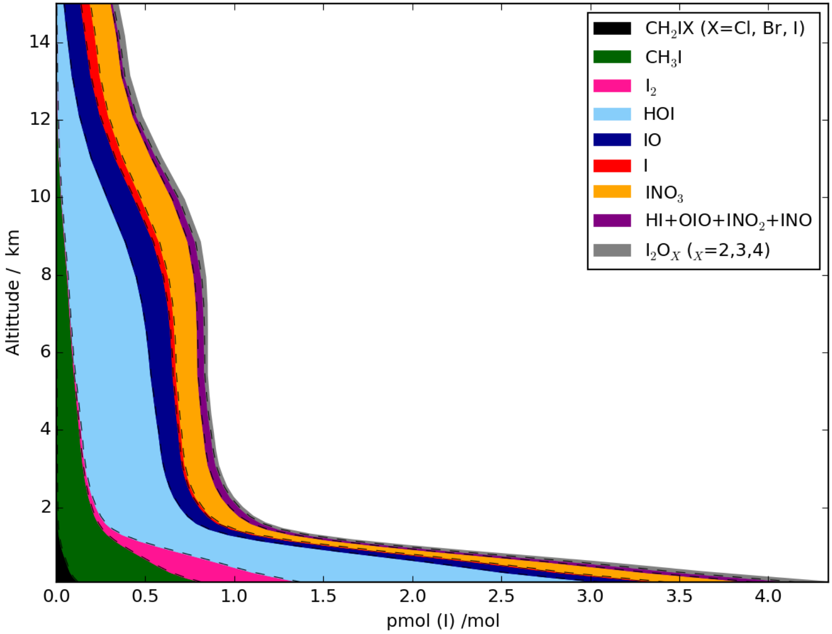

Figure 8. Global annual mean gas-phase iodine speciation with altitude in the simulation with both iodine and bromine chemistry ("Br+I"). Mixing ratios are shown in ~~pptv~~pmol/mol, with higher iodine oxides (I_2O_X (~~$X = 2,3,4$~~$_{X = 2,3,4}$)) and di-halogenated organics (CH_2IX (X = Cl, Br, I)) grouped.

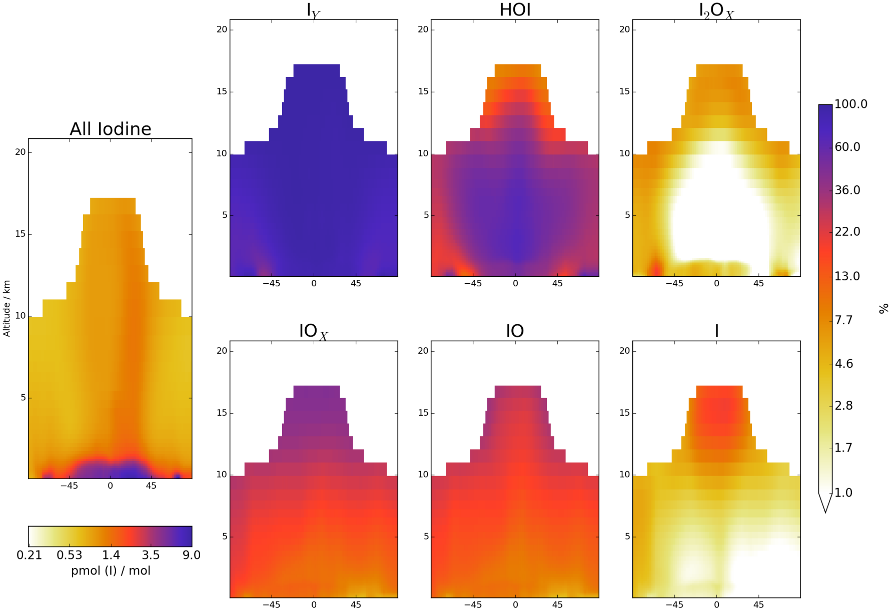

Figure 9. Zonal breakdown of global annual mean iodine speciation by family in the "Br+I" simulation. First panel shows total gas phase iodine concentration and the following panels show percentage of different compounds to this. Total gas phase iodine $= CH_3I + 2CH_2I_2 + CH_2IBr + CH_2ICl + 2I_2 + HOI + IO + OIO + HI + INO_2 + INO_3 + 2I_2O_2 + 2I_2O_3 + 2I_2O_4 + I + INO$; $I_Y = 2I_2 + HOI + IO + OIO + HI + INO + INO_2 + INO_3 + 2I_2O_2 + 2I_2O_3 + 2I_2O_4$; $IO_X = I + IO$.

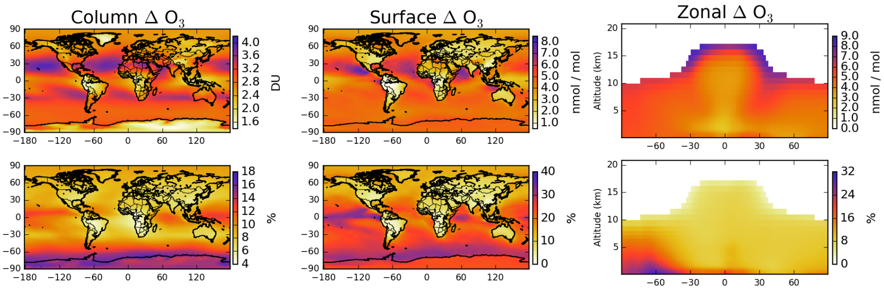

Figure 10. Decreases in annual mean tropospheric column, surface and zonal O_3 with inclusion of iodine ("Br+I"-"BROMINE") chemistry are shown on left, middle and right panels respectively. Upper panels show changes in Dobson units or ~~ppbv~~ nmol/mol and lower panels show changes in percentage terms.~~This is calculated as the difference in the concentrations between standard GEOS-Chem (v9-2, including bromine) and the iodine simulation.~~

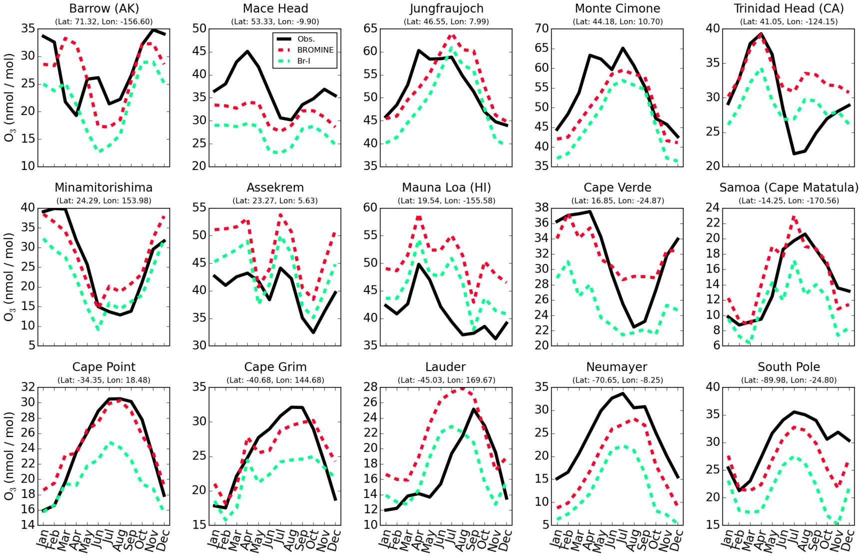

Figure 11. Seasonal cycle of near-surface O_3 at a range of Global Atmospheric Watch (GAW) sites (Sofen et al., 2015). Observational data shown is a 6 year monthly average (2006–2012). Model data is for 2005. Data is from GAW compile and processed as described in (Sofen et al., 2015). Red indicates standard GEOS-Chem (v9-2~~,~~) including bromine chemistry (“BROMINE”) and green with inclusion of iodine chemistry (“Br+I”).

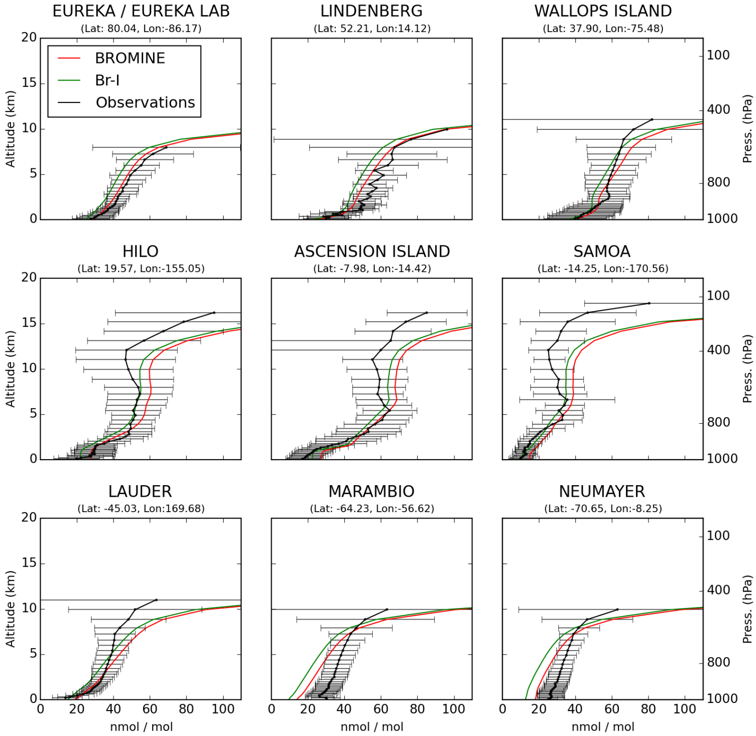

Figure 12. Comparison between annual modelled O_3 profiles and sonde data (2005,WOUDC, 2014). Profiles shown are the annual mean of available observations from World Ozone and Ultraviolet Radiation Data Centre WOUDC (2014) and model data for 2005 at given locations. ~~The~~ Red indicates standard GEOS-Chem (v9-2) including bromine chemistry (“BROMINE”) and ~~the iodine simulation are shown in red and~~ green ~~respectively~~with inclusion of iodine chemistry (“Br+I”). Observations (in black) show mean concentrations with upper and lower quartiles given by whiskers.

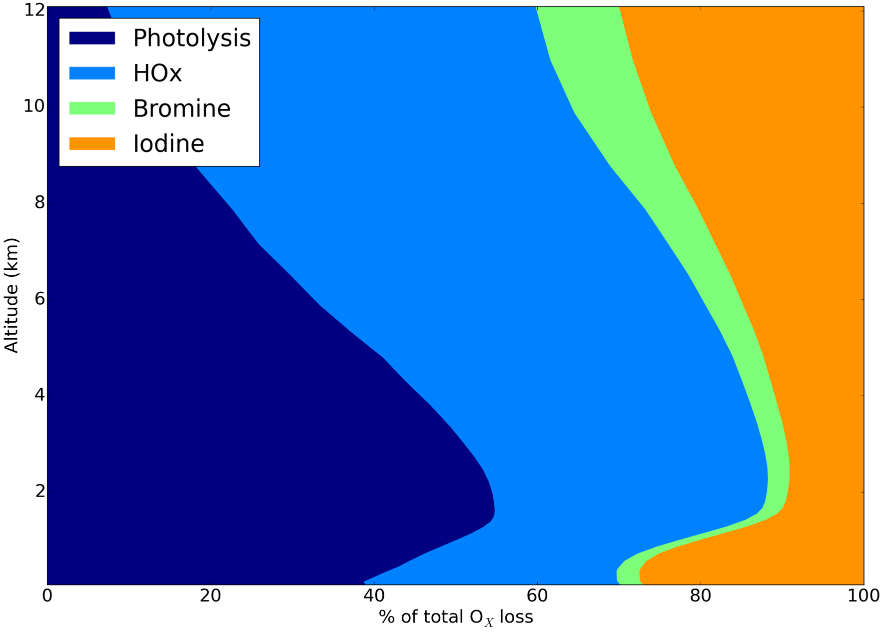

Figure 13. Vertical profile of simulated fractional global annual mean O_X loss by route in the “Br+I” simulation. O_X definition is given in ~~text~~Footnote 1) . Photolysis represents loss of O_X due to O_3 photolysis in the presence of water vapour. HO_X loss includes routes via minor NO_X channels. The magnitude of the bromine route is probably underestimated as discussed in Sect. 2.6.

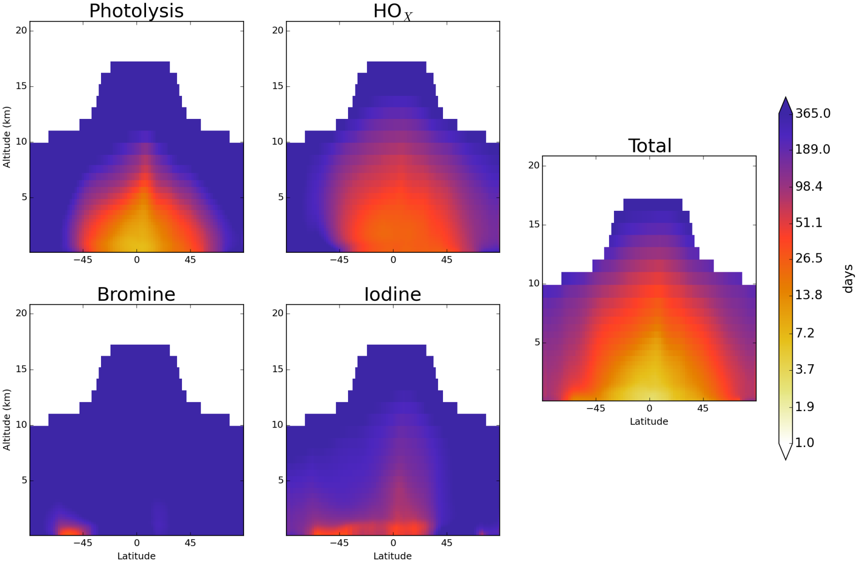

Figure 14. Global annual O_3 mean zonal chemical lifetime for different O_X loss routes (Photolysis, HO_X, Iodine, Bromine, and Total) in the “Br+I” simulation. Values are shown on a log on a scale.

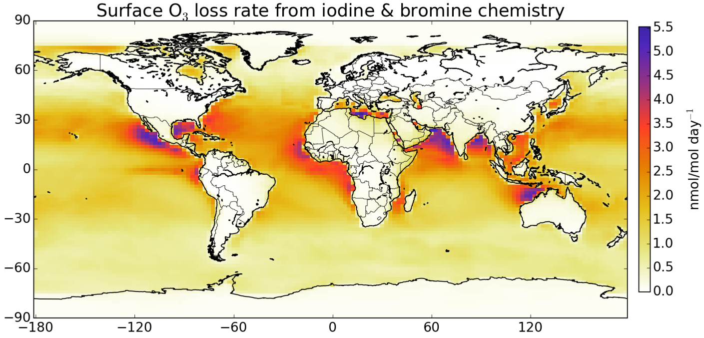

Surface O_3 loss rate from iodine & bromine chemistry

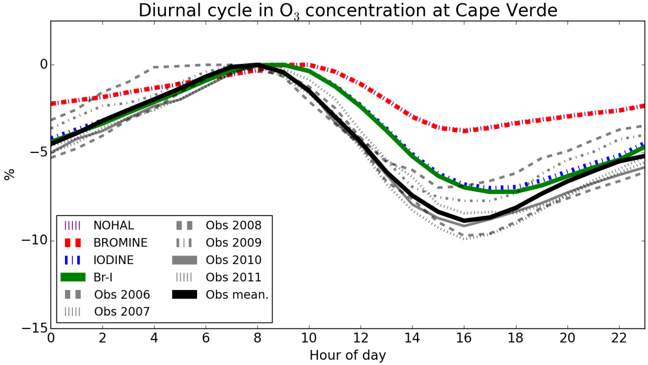

Diurnal cycle in O_3 concentration at Cape Verde

Figure 15. Global annual mean surface O_3 loss (~~ppbv~~ nmol/mol day^{-1}) in the "Br+I" simulation from both bromine and iodine ~~compared to a simulation with neither~~ (top)~~, comparison~~. Comparison between modelled and observed fractional diurnal O_3 cycles at the Cape Verde Observatory for ~~4~~ "NOHAL", "BROMINE", "IODINE" and "Br+I" simulations (bottom). ~~The diurnal change~~ Calculation is ~~calculated by subtracting each day's maximum concentration from the observations (2006–2012), then dividing by the daily means to give a diurnal fraction~~described in text Section . Diurnal changes are averaged over the whole dataset. Lines are black, purple, red, ~~turquoise, green~~ blue and ~~magenta~~ green for mean of observations, "~~no hal~~NOHAL", ~~standard GEOS-Chem (v9-2)~~"BROMINE", "~~just iodine~~IODINE" and ~~iodine simulation~~ "Br+I" respectively. Individual years of observational data are shown in grey.

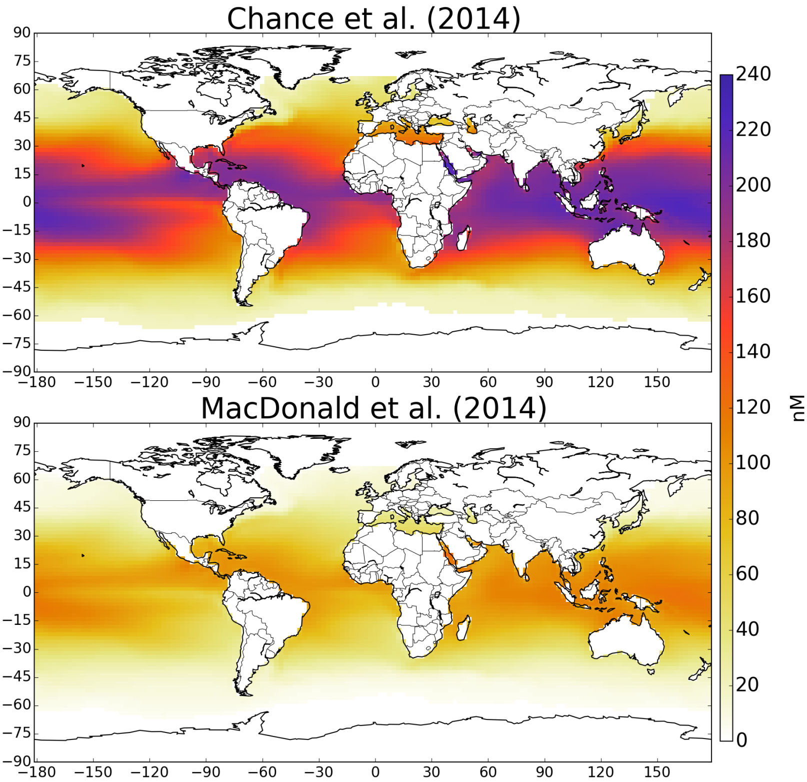

Figure 16. Calculated annual mean ocean surface iodide concentrations (I^-) in nM. Values are calculated from the highest correlation relationship (square) presented in Chance et al. (2014) Table 2 (top) and from Arrhenius relationship from Eq. (1) in MacDonald et al. (2014) (bottom). The Chance et al. (2014) parameterisation is used as the standard in the work with the MacDonald et al. (2014) used as the "Ocean iodide" sensitivity simulation in Sect. 7.

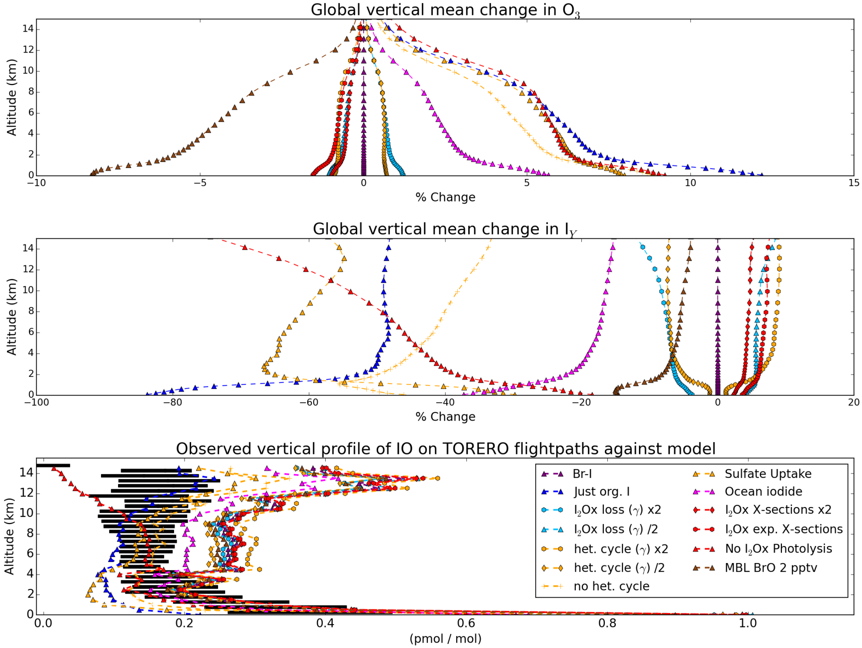

Global vertical mean change in O_3

Global vertical mean change in I_Y

Observed vertical profile of IO on TORERO flightpaths against model

Figure 17. Sensitivity impacts. Upper and middle panels show global mean vertical percentage changes in concentrations of O_3, and I_Y. Lower panel gives vertically averaged iodine oxide (IO) mixing ratios (~~pptv~~pmol/mol) calculated along the TORERO aircraft Volkamer et al. (2015); Wang et al. (2015) flightpaths. The legend (bottom) is shared by all plots. The boxplot of IO observations (black) represents the quartiles of the data, with the median shown within the box.